



# RESEARCH MEMORANDUM

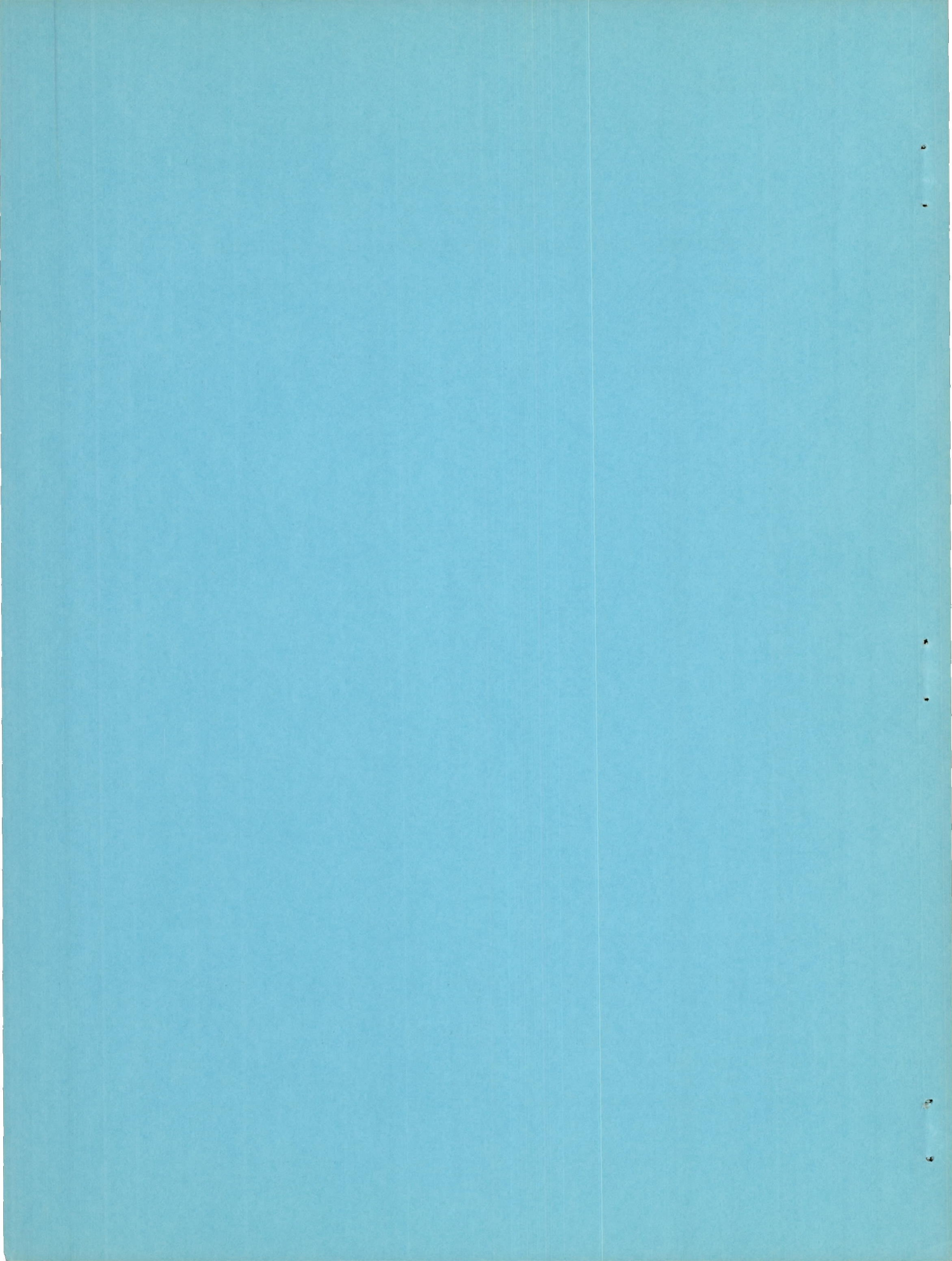
AERODYNAMIC LOADING CHARACTERISTICS OF A WING-FUSELAGE  
COMBINATION HAVING A WING OF  $45^{\circ}$  SWEEPBACK MEASURED  
IN THE LANGLEY 8-FOOT TRANSONIC TUNNEL

By Donald L. Loving and Claude V. Williams

Langley Aeronautical Laboratory  
Langley Field, Va.

NATIONAL ADVISORY COMMITTEE  
FOR AERONAUTICS  
WASHINGTON

May 19, 1952  
Declassified February 26, 1958



## NATIONAL ADVISORY COMMITTEE FOR AERONAUTICS

## RESEARCH MEMORANDUM

## AERODYNAMIC LOADING CHARACTERISTICS OF A WING-FUSELAGE

COMBINATION HAVING A WING OF  $45^\circ$  SWEEPBACK MEASURED

## IN THE LANGLEY 8-FOOT TRANSONIC TUNNEL

By Donald L. Loving and Claude V. Williams

## SUMMARY

An investigation of the aerodynamic loading characteristics of a wing-fuselage combination was conducted in the slotted test section of the Langley 8-foot transonic tunnel. The model had a wing with  $45^\circ$  sweepback of the 0.25-chord line, an aspect ratio of 4, a taper ratio of 0.6, and NACA 65A006 airfoil sections parallel to the plane of symmetry, and was mounted in the midwing position on the general transonic fuselage. The test was part of a systematic investigation of the effects of varying the amount of sweepback on wings in order to determine their suitability for transonic flight. The data obtained in the slotted transonic test section bridge the gap in wind-tunnel data which had heretofore been unobtainable between Mach numbers of approximately 0.96 and 1.2 in the closed-throat test section of the Langley 8-foot high-speed tunnel.

The largest changes with Mach number in the aerodynamic characteristics occurred in the transonic speed range between Mach numbers of 0.90 and 1.02. The spanwise load on the wing at a given angle of attack was characterized by outboard shifts in lateral center of pressure with increase in Mach number. There was a rearward shift in chordwise center of pressure and large increases in the pitching-moment coefficient in a negative direction through the transonic speed range. A loss in load over the outboard sections of the wing, which occurred with an increase in angle of attack and was due to separation, was delayed to higher angles of attack as the Mach number was increased.

The load on the fuselage and inboard sections of the wing increased with an increase in angle of attack at all Mach numbers. The percentage of total load carried by the fuselage at low angles of attack was approximately equal to the percentage of total wing area blanketed by the fuselage. The percentage of total load carried by the fuselage at higher angles of attack exceeded the percentage of wing area blanketed by the fuselage by an increasing amount as the angle of attack was increased.

## INTRODUCTION

The installation of the slotted transonic test section in the Langley 8-foot high-speed tunnel has made it possible to conduct aerodynamic investigations at Mach numbers through the speed of sound without the usual effects of choking and blockage associated with closed-throat wind tunnels. The problem of wave reflections from the tunnel walls onto the model still exists, but data are not presented herein for the conditions at which they occur. Extensive pressure measurements on a wing-fuselage combination having a wing of  $45^\circ$  sweepback were obtained at transonic speeds in the recently installed slotted test section. The basic pressure measurements in the form of pressure coefficients have been reported in reference 1. The data obtained in the slotted transonic test section bridge the gap in wind-tunnel data which had heretofore been unobtainable between Mach numbers of approximately 0.96 and 1.2 in the closed-throat test section of the Langley 8-foot high-speed tunnel. Measurements were made at angles of attack of  $4^\circ$ ,  $8^\circ$ , and  $12^\circ$  for the same wing-fuselage combination tested in the closed-throat test section and reported in reference 2. Tests also were made in the slotted test section at an angle of attack of  $20^\circ$  through the Mach number range from 0.60 to 1.11. Force test results for the same configurations tested in the closed-throat test section have been reported in reference 3.

A more detailed analysis of the pressure-distribution data obtained in the slotted test section (reference 1) is presented herein in terms of section and over-all wing-fuselage characteristics.

The Reynolds number for this investigation varied from  $1.73 \times 10^6$  to  $2.01 \times 10^6$  when based on the wing mean aerodynamic chord or from  $9.44 \times 10^6$  to  $10.95 \times 10^6$  when based on fuselage length.

## SYMBOLS

b	wing span
c	airfoil section chord, parallel to plane of symmetry
$\bar{c}$	average wing chord (S/b)
c'	mean aerodynamic chord $\left( \frac{2}{S} \int_0^{b/2} c^2 dy \right)$

d	fuselage section diameter
$d_{\max}$	fuselage maximum diameter
M	Mach number
p	free-stream static pressure
$p_l$	local static pressure
P	pressure coefficient $\left(\frac{p_l - p}{q}\right)$
q	free-stream dynamic pressure $\left(\frac{1}{2} \rho V^2\right)$
R	Reynolds number $\left(\frac{\rho V c'}{\mu}\right)$
r	fuselage section radius
S	total wing area
V	velocity in undisturbed stream
x	distance measured parallel to the plane of symmetry from leading edge of section
y	distance measured perpendicular to the plane of symmetry in spanwise direction
$\alpha$	angle of attack of fuselage center line
$\theta_t$	angle of twist of wing tip, measured parallel to plane of symmetry
$\rho$	mass density in undisturbed stream
$\mu$	coefficient of viscosity in undisturbed stream

## Subscripts:

f	fuselage cross section
L	lower surface of section
U	upper surface of section

The coefficients are defined as follows:

$C_b$  bending-moment coefficient of the wing outside the fuselage about the wing-fuselage juncture

$$\left( \frac{2}{b \left( \frac{b}{2} - \frac{d_{\max}}{2} \right)} \int_{d_{\max}/2}^{b/2} \frac{c_{nc}}{c} y \, dy \right)$$

$C_n$  wing-section normal-force coefficient  $\left( \frac{1}{c} \int_0^c (P_L - P_U) \, dx \right)$

$\frac{c_{nc}}{c}$  section normal-loading coefficient

$C_{nf}$  fuselage cross-section normal-force coefficient

$$\left( \frac{1}{2r} \int_{-r}^r (P_L - P_U) \, dy \right)$$

$\frac{C_{nf} d}{d_{\max}}$  fuselage cross-section normal-loading coefficient

$C_N$  normal-force coefficient of wing-fuselage combination

$C_m$  section pitching-moment coefficient about 25-percent-chord

position  $\left( \frac{1}{c^2} \int_0^c (P_U - P_L) \left( x - \frac{c}{4} \right) \, dx \right)$

$C_m$  pitching-moment coefficient of wing-fuselage combination about 25-percent-mean-aerodynamic-chord position

## APPARATUS AND METHODS

### Tunnel

The investigation was conducted in the slotted test section of the Langley 8-foot transonic tunnel. This facility is a single-return wind tunnel having a dodecagonal, slotted throat in which the Mach number is continuously variable through the subsonic speed range, at and through the speed of sound, and at supersonic speeds up to a Mach number of

approximately 1.14. Explorations of the flow in the slotted test section indicated that uniform flow exists throughout the speed range of the tunnel. The design and calibration of this transonic testing facility have been reported in references 4 and 5. At free-stream Mach numbers below 1.03, deviations in Mach number did not exceed 0.003. At Mach numbers above 1.03 the maximum deviations from the average stream Mach numbers increased gradually to a value not exceeding 0.010. Further investigation of the flow in the tunnel revealed that the angularity of the flow in the test section was approximately  $0.1^\circ$ . All data were obtained at corrected angles of attack to compensate for this angularity.

### Model

The model investigated was the same as that tested in the closed-throat test section of the Langley 8-foot high-speed tunnel. A complete description of the model may be found in reference 2. The wing had the quarter-chord line swept back  $45^\circ$ , an aspect ratio of 4, a taper ratio of 0.6, and NACA 65A006 airfoil sections parallel to the plane of symmetry, and was mounted on the fuselage in the midwing position. Dimensional details of the wing-fuselage combination are presented in figure 1. The wing was constructed of a steel core (see table I) with the external contour of the sections formed by a tin-bismuth alloy covering. One hundred and fifteen static-pressure orifices were located in the upper and lower surfaces of the wing, distributed among five spanwise stations parallel to the plane of symmetry (20-, 60-, and 95-percent semispan on the left wing; and 40- and 80-percent semispan on the right wing). The steel fuselage had a circular cross section and a basic fineness ratio of 12, which was modified to an actual fineness ratio of 10 by cutting off one-sixth of the fuselage to attach the sting. One hundred and eight static-pressure orifices were distributed among six meridians on the fuselage, designated by A, B, C, D, E, and F, from the upper to the lower surface (fig. 1). A photograph of the model mounted in the slotted test section of the tunnel is presented as figure 2.

An attempt was made to maintain the model aerodynamically smooth throughout the investigation; however, the lower surface of the wings became badly pitted and rough at the high angles of attack because of dirt particles in the air stream.

### Model Support System

The model was supported by a tapered sting attached to the rear of the fuselage. The tapered sting was mounted on a support tube which was fixed axially in the center of the tunnel by two sets of supports projecting from the tunnel walls. The forward tapered portion of the support tube was hinged to the rear portion in such a manner that the

angle of attack could be changed while the tunnel was operating. Details of the model support system and the model location in the slotted transonic test section are shown in figures 3 and 4.

#### Measurements

The angle of attack of the model was measured by sighting the cross-hair of a cathetometer on a reference line marked on the fuselage. The use of this device in conjunction with the remotely controlled angle-of-attack changing mechanism enabled model angles of attack to be set to within  $\pm 0.1^\circ$  with the tunnel operating at any Mach number.

The same cathetometer was used to sight on a reference line marked on the tip of the wing. This measurement provided information on the angle of twist of the wing tip. Because of the vibrations of the wing tip during the investigation, the measurements of wing-tip twist are judged to be accurate only to within  $\pm 0.25^\circ$ .

#### Tests

The investigation was planned to accomplish two purposes. The first purpose was to obtain aerodynamic information in the Mach number range between 0.96 and 1.2 which heretofore could not be obtained in the closed-throat test section of the Langley 8-foot high-speed tunnel. The angles of attack to be tested were selected in order to cover the more representative angles of attack of those tested in the earlier investigation reported in reference 2. The second purpose was to cover the speed range from a Mach number of 0.60 to the highest obtainable Mach number at an angle of attack considered to be in the region near maximum lift. Tests were made for angles of attack up to  $20^\circ$  at Mach numbers from 0.60 to 1.13. The basic pressure distributions for all angles of attack tested are presented in reference 1. The analysis of the data for the following angles of attack and Mach numbers are presented herein:

Angle of attack (deg)	Mach number
4	0.94, 0.97, 0.99, 1.02, 1.11, 1.13
8	0.94, 0.97, 0.99, 1.02, 1.11, 1.13
12	0.89, 0.94, 0.97, 0.99, 1.02, 1.11, 1.13
20	0.60, 0.79, 0.89, 0.94, 0.97, 0.99, 1.02, 1.11

The variation with Mach number of the approximate test Reynolds number based on the wing mean aerodynamic chord of 6.125 inches is presented in figure 5.

## RESULTS

The section and over-all wing-fuselage characteristics were obtained from graphical integrations of the basic pressure measurements described in reference 1. The results are presented for angles of attack of  $4^\circ$ ,  $8^\circ$ ,  $12^\circ$ , and  $20^\circ$ . These angles of attack were selected as representative of the angles of attack at which the more important aerodynamic phenomena occur. Data for angles of attack of  $4^\circ$ ,  $8^\circ$ , and  $12^\circ$  obtained in the closed-throat test section of the Langley 8-foot high-speed tunnel at subsonic speeds up to a Mach number of 0.96 and at a supersonic Mach number of 1.2 (reference 2) are included. These data are utilized to present the complete variation with Mach number of the various parameters presented herein.

The spanwise distribution of the section normal-loading coefficients and the section pitching-moment coefficients presented for the fuselage in the presence of the wing were obtained from several vertical planes which pass through the fuselage. These section normal-loading coefficients were based on the chords of the sections of the wing extended into the fuselage. The section pitching-moment coefficients were based on the quarter chords of these same sections.

Mutual interference effects of the wing on the fuselage and the fuselage on the wing are present in the results since they were obtained from the investigation of the wing-fuselage combination.

Symbols are used on the figures to indicate the data obtained during the present investigation in the slotted test section. The solid lines without symbols indicate the results of the previous investigation made in the closed-throat test section (reference 2). The tunnel wall interference due to wave reflections modified the flow over the model, therefore, data are not given for the range of Mach numbers from 1.02 to 1.11 in order to ensure that the data presented are free of these effects. The data shown for a Mach number of 1.2 were obtained from the investigation in the closed-throat test section for an angle of attack of  $4^\circ$  only.

## DISCUSSION

Frequent reference to the basic pressure measurements presented in reference 1 may be desirable in conjunction with the discussion of the aerodynamic characteristics presented herein.

## Span Load Characteristics

The spanwise distribution of load on the model is presented in terms of section normal-loading coefficient  $\frac{c_n^c}{c}$  in figures 6(a) to 6(i). In figures 6(a) to 6(c) the loading on the fuselage is the average of the section normal-loading coefficients on the fuselage for Mach numbers from 0.60 to 0.90. The load distributions in figures 6(d) to 6(i) are shown for the complete semispan of the model beginning at the vertical center line of the fuselage and extending out to the tip of the wing. In this manner the actual load carry-over from the wing to the fuselage is portrayed for the various angles of attack tested at Mach numbers from 0.94 to 1.13. The average of the section loadings on the fuselage is presented in figures 6(a) to 6(c) rather than the individual section loadings because of the time involved in computing the individual section loadings. The shape of the spanwise distribution of loading over the fuselage is well established for the more important Mach number range between 0.94 and 1.13 in figures 6(d) to 6(i).

Several general characteristics in the spanwise load distribution are immediately apparent. The section loading coefficient over the fuselage and inboard sections of the wing increased with an increase in angle of attack up to  $20^\circ$ . The loading on the outboard sections increased with change in attitude up to the angle of attack at which severe separation was experienced over this region of the wing. The point at which severe separation occurred over the wing tip was indicated to be delayed to higher angles of attack as the Mach number was increased. The spanwise distribution of loading did not change appreciably with increase in Mach number from 0.60 to 0.80. Thereafter the loading shifted outboard with increase in Mach number, except for an angle of attack of  $12^\circ$  at a Mach number of 0.90; at this condition a slight inboard shift was noted due to the severe separation over the outboard sections.

The results of reference 2 and of the present investigation indicate that a dip in the spanwise load distribution, corresponding to a reduction in load occurred between the fuselage center line and the wing-fuselage juncture (fuselage maximum diameter). This discontinuity in loading became larger with increase in angle of attack from  $4^\circ$  to  $20^\circ$ .

Angle of attack of  $4^\circ$ .- At an angle of attack of  $4^\circ$  and Mach numbers up to 0.94 (figs. 6(a) to 6(d)) the spanwise distribution of section normal-loading coefficient was characterized by a nearly elliptical shape, as might be expected from theory. Increasing the Mach number to 0.99 caused that part of the load carried by the outboard regions of the wing to increase, while that carried by the inboard sections decreased (figs. 6(e) and 6(f)). This trend with increase in Mach number resulted in a roughly rectangular loading over the wing at Mach numbers of 0.99 and 1.02, where the level in loading at the 80-percent station was approximately the same as the level in loading at the 20-percent station. When the Mach number was increased from 1.02 to 1.13 (figs. 6(g) to 6(i)) the distribution of load returned to approximately that indicated at the subsonic Mach number of 0.97. Throughout the Mach number range from 0.94 to 1.13 the value of normal loading coefficient at the tip region (95-percent semispan station) remained almost constant at a value on the order of 0.21.

Angle of attack of  $8^\circ$ .- At an angle of attack of  $8^\circ$  the variation of spanwise loading with increasing Mach number was essentially the same as that indicated at an angle of attack of  $4^\circ$ , although more pronounced. For example, increasing the Mach number from 0.94 to 0.99 resulted in a decrease in the load carried by the inboard sections and an appreciable increase in the load over the outboard regions. This created a peak in the distribution located in the region of the 80-percent semispan station. The shape of the spanwise load distribution remained about the same at the higher Mach numbers but the values of section normal-loading coefficient decreased slightly with increase in Mach number indicating a slight reduction in over-all load on the wing.

Angle of attack of  $12^\circ$ .- Between angles of attack of  $8^\circ$  and  $12^\circ$  at Mach numbers up to 0.94 a marked change in the nature of the air flow over the wing produced a pronounced change in the distribution of load over the wing span. At  $12^\circ$  angle of attack it was evident that severe separation of the flow over the outer sections of the wing resulted in a considerably smaller amount of the total load being carried by this region than at the lower angles of attack. The most evident loss of loading, as the angle of attack was increased to  $12^\circ$ , occurred at Mach numbers between 0.89 and 0.94. At the same time the load over the fuselage and the inboard stations of the wing continued to increase with increase in angle of attack. Increasing the Mach number above 0.94 caused the level of loading on the outboard regions of the wing to gradually increase until at Mach numbers of 1.11 and 1.13 the distributions were much the same as those of the lower angles of attack of  $4^\circ$  and  $8^\circ$ . This increase of loading on the outboard stations was associated with the delay in the separation over the outboard stations to higher angles of attack as the Mach number was increased.

Angle of attack of 20°.- At 20° angle of attack and Mach numbers up to 0.99 the distribution of load over the wing was roughly triangular in shape and was indicative of the inboard spread of separated flow over the wing as angle of attack was increased beyond 8°. The distribution was much the same as for 12° except that the maximum value of wing section normal-force coefficient occurred at the 20-percent semispan station rather than the 40-percent semispan station. With increase in Mach number, changes in the load distribution were noted for the inboard stations only. Here the loading was seen to shift outboard in the same manner as for the sections nearer the wing tip at lower angles of attack.

### Normal-Force Characteristics

Total normal-force coefficient.- The variation with Mach number of the total normal-force coefficient,  $C_N$ , presented in figure 7, is the summation of all the section normal-loading coefficients acting on the wing-fuselage combination. The values of the total normal-force coefficients obtained from the slotted-throat investigation continued without discontinuity the trends with Mach number indicated by the values obtained from the closed-throat investigation, except for an angle of attack of 4°. At an angle of attack of 4°, the discontinuity is believed to be due in part to an inaccuracy in the 4° angle of attack of the model when investigated in the closed-throat test section.

For an angle of attack of 4° the normal-force coefficient appeared to reach a maximum value of 0.35 at a Mach number of approximately 0.95. At angles of attack above 4° the normal-force coefficient increased in the Mach number range between 0.90 and 1.00. The rate of increase became greater as the angle of attack was increased from 8° to 20°. The force break Mach number also was delayed to higher values as the angle of attack was increased. The maximum normal-force coefficient value of 1.14 occurred for an angle of attack of 20° at the force break Mach number of 1.025. The normal-force coefficients for Mach numbers of 1.11 and 1.13, at all angles of attack, were slightly less than the values obtained at the force break.

Percent of total load carried by fuselage.- At an angle of attack of 4° the percent of the total load carried by the fuselage, as shown in figure 8, remained relatively constant throughout the Mach number range investigated and is on the order of 16 percent. These data indicate that, at least for the low angles of attack, the fuselage carried about the same proportion of the total load as would be carried by the portion of the wing blanketed by the fuselage, if the fuselage were not present. For this wing-fuselage combination 16.5 percent of the total wing area was covered by the fuselage.

At all Mach numbers the percentage of total load carried by the fuselage increased with increasing angle of attack above  $8^\circ$ . For example, at an angle of attack of  $8^\circ$  and a Mach number of 1.11 the fuselage carried 13.6 percent of the total load, whereas at an angle of attack of  $20^\circ$  for the same Mach number the load carried by the fuselage relative to the total load increased to 19.1 percent. This increase was associated with the inboard shift of the spanwise load distribution on the wing with increase in angle of attack. The limiting values of the percent of total load carried by the fuselage varied from a minimum of 13.7 percent occurring at an angle of attack of  $8^\circ$  and a Mach number of 1.11, to a maximum value of 23.5 percent at an angle of attack of  $20^\circ$  and a Mach number of 0.60.

Lateral center of pressure.- The variation of lateral position of the center of pressure with Mach number as shown in figure 9 reflects the changes in the spanwise load distribution discussed in connection with figure 6. As might be expected from an examination of the spanwise distribution of loading (fig. 6), the location of the lateral center of pressure at any particular angle of attack was approximately constant from a Mach number of 0.60 to 0.90, moved outboard from a Mach number of 0.90 to 1.00, and was fairly constant at the supersonic Mach numbers. The changes in location of the lateral center of pressure were small with the maximum change being of the order of 10 percent of the semispan outside the fuselage.

The most outboard position of the lateral center of pressure was noted for the Mach numbers in the range from 0.99 to 1.13 for an angle of attack of  $8^\circ$ . For these conditions the center of pressure was located at approximately 48 percent of the semispan outside of the fuselage. This was primarily the result of relatively higher loads over the wing-tip region than those farther inboard.

At an angle of attack of  $20^\circ$ , since the shape of the spanwise load distribution remained approximately the same with increase in Mach number, the lateral position of the center of pressure did not vary appreciably with Mach number. It may be noted also that at an angle of attack of  $20^\circ$  the inboard sections of the wing carried a greater load relative to the outboard sections than at any other angle of attack tested; therefore, as expected, the lateral center of pressure was located at the most inboard position noted during the investigation which was approximately 37 percent of the semispan outside the fuselage at subsonic Mach numbers and 40 percent at the supersonic speeds.

Bending-moment coefficient.- The bending-moment coefficient of the wing about the wing-fuselage juncture is a direct function of the location of the lateral center of pressure and normal force acting on the wing. In figure 10 the values of the bending-moment coefficient increased from 0.08 to 0.10 with an increase in Mach number from 0.60

to 0.85 for an angle of attack of  $4^\circ$ . At  $12^\circ$  angle of attack, for the same Mach numbers, the values of the bending-moment coefficient decreased from 0.23 to 0.22. The bending-moment coefficient increased rapidly with increase in Mach number between 0.90 and 1.00 for all angles of attack above  $4^\circ$ . The values were generally less at a Mach number of 1.11 than 1.00 for angles of attack of  $4^\circ$ ,  $8^\circ$ , and  $20^\circ$ . The maximum value of bending-moment coefficient was 0.37, and this occurred at an angle of attack of  $20^\circ$  at a Mach number of 1.02.

### Wing-Tip Angle of Twist

Positive aerodynamic lifting loads on sweptback wings produce bending along the span with progressively less positive angle of attack of the sections from the wing-fuselage juncture out toward the wing tip. As a result, significantly different spanwise and chordwise loading distributions occur on swept wings of varying rigidity even though they may have the same airfoil sections and geometric dimensions.

An indication of the elasticity of the wing used in the present investigation is given in figure 11 by the measurements of the wing-tip angles of twist for angles of attack of  $4^\circ$ ,  $8^\circ$ ,  $12^\circ$ , and  $20^\circ$ . The minus signs preceding the ordinate values indicate a decrease in angle of attack of the wing tip compared with the fuselage center line. The measurements reflect the variation with Mach number of the loading on the wing for this particular investigation only as tested in the Langley 8-foot transonic tunnel. Measurements on this wing in free flight or other testing facility would be expected to be different from the data presented herein because of differences in the values of the free-stream dynamic pressure  $q$  for the various testing techniques.

The magnitude of the angle of twist of the wing tip increased with increase in both angle of attack and Mach number, reaching a maximum value of  $2.6^\circ$  at an angle of attack of  $20^\circ$  and a Mach number of 1.11. The most rapid change for a given angle of attack occurred for an angle of attack of  $12^\circ$  between Mach numbers of 0.94 and 1.05. The value at a Mach number of 1.05 was 130 percent higher than at a Mach number of 0.94. This was because of the rapid outboard shift in lateral center of pressure as a result of the delay in inboard spread of separation at an angle of attack of  $12^\circ$  when the Mach number was increased from 0.94 to 1.05. At the higher Mach numbers the increase in wing-tip angle of twist was small with increase in angle of attack between  $12^\circ$  and  $20^\circ$  because of the inboard shift in center of pressure (fig. 9) caused by the inboard spread of the region of separated flow at the wing tip.

An attempt was made to calculate the twist of the tip of the wing and to compare the values with the actual experimental measurements

obtained during the investigation. It was assumed that the entire load was carried by the steel core of the wing, that zero bending occurred about the 21-percent semispan station, and that the axis of zero twist was along the 47.5-percent-chord line of the steel core (center of mass of steel-core cross section). (See table I.) The 47.5-percent-chord line of the steel core corresponds to the 48.8-percent-chord line of the airfoil sections. The moment of inertia of a steel-core section perpendicular to the 47.5-percent-chord line about the chord line of that section was calculated to be the product of the chord of the steel core and the cube of the maximum thickness of the steel core divided by 21.66, with a modulus of elasticity of  $30 \times 10^6$  pounds per square inch. These assumptions, in conjunction with the spanwise loading distributions shown in figure 6(a) to 6(i), were used in the application of the moment-area method for determining the angle of twist of the wing tip.

Calculated angles of twist of the wing tip for angles of attack of  $12^\circ$  and  $20^\circ$  are compared with the measured values in figure 11. The calculated angles agree satisfactorily with experiment in the manner of variation with Mach number, but exceed the magnitude of the measured values. Overestimation is to be expected since the tin-bismuth alloy covering, pressure tubes, and other machined characteristics of the wing were not considered in the estimation of the moment of inertia of the steel-core cross sections. Nevertheless, the calculated values do show that the trend with angle of attack and Mach number of the wing-tip twist angle due to bending may be predicted with reasonable accuracy if the spanwise load distribution is known.

#### Spanwise Distribution of Section Pitching-Moment Coefficient

The section pitching-moment coefficients about the quarter chord of the wing sections are presented in figures 12(a) to 12(c) for the semispan of the wing outside the fuselage at Mach numbers from 0.60 to 0.90, for various angles of attack. The spanwise distribution of section pitching-moment coefficient for Mach numbers from 0.94 to 1.13 (figs. 12(d) to 12(i)) is shown for the complete semispan of the model extending from the vertical center line of the fuselage to the wing tip.

The fuselage section pitching-moment coefficients were characterized by large changes from positive to negative values in the spanwise direction from the vertical center line of the fuselage. These extreme conditions were magnified by increases in angle of attack.

Large changes in the shape of the distribution of section pitching-moment coefficient over the wing semispan occurred when the angle of attack was increased at any particular Mach number. For example, as the angle of attack was increased from  $4^\circ$  to  $8^\circ$ , a region of negative

pitching-moment coefficient occurred at the outboard section of the wing due to an increase in the chordwise extent of relatively high negative pressure coefficients over this outer section. With continued increase in angle of attack, the region of most negative section pitching-moment coefficient was seen to shift inboard. This shift resulted from increases in the level of negative pressure coefficient over the trailing edge of inboard sections of the wing and the onset of separation over the outboard sections. Once separation was established in the flow over the wing sections, change in angle of attack had little effect on change in pitching-moment coefficient of these stalled sections.

The delay in inboard spread of negative section pitching-moment coefficient at the higher Mach numbers was due to the delay in inboard spread of separation with increase in Mach number. A similar delay has been discussed with regard to the spanwise distribution of section normal-loading coefficient.

#### Pitching-Moment Characteristics

Total pitching-moment coefficient.- The values of pitching-moment coefficient (fig. 13) obtained in the slotted test section at transonic speeds for the wing-fuselage combination continue without discontinuity the trends with Mach number obtained in the closed-throat investigation of the same combination.

In general, the variations with Mach number of the pitching-moment coefficient for the wing-fuselage combination, as shown in figure 13, were influenced mostly by the pitching-moment characteristics of the wing, since at any particular angle of attack within the speed range of this investigation the pitching moment for the fuselage is indicated by the pressure distributions in reference 1 to be relatively constant. The pitching-moment coefficients for the wing-fuselage combination were characterized by large increases in pitching-moment coefficients in a negative direction at transonic speeds up to a Mach number of 1.02. These negative pitching-moment-coefficient gradients were the result principally of rearward shifts in the chordwise center of pressure on the wing-fuselage configuration (fig. 14). These rearward shifts are caused by the shift of load along the wing toward the tip sections (fig. 9) as well as by rearward shifts in section loading. Most of the shift occurred in the speed range between Mach numbers 0.89 and 1.02. At Mach numbers of 1.11 and 1.13 the pitching moment appeared to differ little from the values at a Mach number of 1.02, except at an angle of attack of  $12^\circ$ ; at this angle of attack the pitching-moment coefficients became more negative, as might be expected from the continued rearward shift in center of pressure and from maintenance of normal force on the wing at Mach numbers up to 1.13.

Generally, increasing the angle of attack from  $4^\circ$  to  $20^\circ$  delayed the break in the pitching-moment-coefficient curves toward more negative values to a higher Mach number. For example, at an angle of attack of  $8^\circ$  the pitching-moment-coefficient curve broke in a negative direction at a Mach number of approximately 0.85, while at an angle of attack of  $20^\circ$  the break was delayed until a Mach number on the order of 0.925 was reached.

Chordwise center of pressure of wing outside of fuselage.- The location of the chordwise center of pressure is a function of not only the chordwise distribution of section loading, but the spanwise distribution of section loading as well. The variation of chordwise center of pressure with Mach number (fig. 14) was shown to be fairly constant from a Mach number of 0.60 to 0.90, moved gradually rearward between Mach numbers of 0.90 and 1.00, and was approximately constant in the supersonic speed range. As a typical example, the chordwise center of pressure for an angle of attack of  $4^\circ$  was located at about 37 percent of the mean aerodynamic chord between Mach numbers of 0.60 and 0.89. When the Mach number was increased to 1.02 the center of pressure shifted rearward to 51 percent of the mean aerodynamic chord and remained at this approximate location up to a Mach number of 1.2.

Longitudinal center-of-pressure location of the wing-fuselage combination.- The longitudinal center-of-pressure location of the wing-fuselage combination, relative to the leading edge of the mean aerodynamic chord (fig. 15), shows the same trends with increase in Mach number and angle of attack as was shown by figure 14 for the wing characteristics outboard of the fuselage. The most pronounced changes in the location of the center of pressure occurred in the Mach number range between 0.85 and 1.02. The changes were in the form of rapid rearward movements of the center of pressure, averaging on the order of 15 percent of the mean aerodynamic chord with increase in Mach number. At a Mach number of 0.60 the center of pressure was located at approximately 20 percent of the mean aerodynamic chord for angles of attack of  $4^\circ$  and  $20^\circ$ . At a Mach number of 1.02 for these same angles of attack the center of pressure shifted to approximately 36 and 30 percent of the mean aerodynamic chord, respectively.

Aerodynamic center.- The location of the aerodynamic center (fig. 16) is presented for the range of normal-force coefficients usually associated with the normal maneuvering flight of an aircraft of this configuration (values of  $C_N$  from 0.2 to 0.6). At Mach numbers up to 0.80 the location of the aerodynamic center was relatively constant at approximately the 25-percent station of the mean aerodynamic chord for normal-force coefficients of 0.2 and 0.4, and at the 20-percent station for a normal-force coefficient of 0.6. Increasing the Mach number from 0.80 to 1.02 caused a rapid rearward shift in the location of the aerodynamic

center with the maximum change in location occurring for a normal-force coefficient of 0.6. For this normal-force coefficient the aerodynamic center moved from the 20.5- to the 50-percent station of the mean aerodynamic chord. At a Mach number of 1.02 for normal-force coefficients from 0.2 to 0.6 the aerodynamic center was at its most rearward location, 50 percent of the mean aerodynamic chord, and remained at approximately the same station with increase in Mach number from 1.02 to the maximum Mach number of 1.2 of this investigation.

### Fuselage Characteristics in Presence of Wing

Fuselage longitudinal-load coefficient.- The distributions of longitudinal loading on the fuselage, presented in figure 17, are expressed in terms of fuselage cross-section normal-loading coefficient  $\frac{c_{n_f} d}{d_{max}}$ .

From these distributions it is evident that the presence of the wing greatly influenced the load distribution over the fuselage, especially at the region of the wing-fuselage juncture. At the subsonic Mach numbers this effect of the wing was evident in front of and behind the wing-fuselage juncture. Increasing the Mach number from 0.94 to 1.13 for this investigation resulted in a decrease in the influence of the wing ahead of the wing-fuselage juncture, a broadening of the influence of the wing behind the juncture, a rise in the loading level over the rear part of the wing-fuselage juncture at an angle of attack of  $20^\circ$ , and a gradual reduction in the maximum values of loading over the fuselage in the region of the wing location.

The most pronounced changes in the distribution were those produced by varying the angle of attack. As the angle of attack was increased from  $4^\circ$  to  $20^\circ$  at a Mach number of 0.94, the values of the fuselage cross-section normal-loading coefficient increased from 0.275 to 0.965 in the region of the wing-fuselage juncture. At a Mach number of 1.11 slightly lower levels of maximum fuselage cross-section normal-loading coefficient were obtained for the angles of attack investigated.

Longitudinal center-of-pressure location of the fuselage in the presence of the wing.- The location of the longitudinal center of pressure of the loads on the fuselage in the presence of the wing is expressed in terms of percent of the fuselage length in figure 18. The center-of-pressure shifts on the fuselage were due primarily to the chordwise shifts in loading on the sections of the wing adjacent to the fuselage. At Mach numbers up to 0.80 the center of pressure was located approximately at the 45 percent point of the fuselage length. Increasing the Mach number up to 1.00 resulted in a relatively rapid rearward shift to approximately 48 percent of the fuselage length. At supersonic speeds the center of pressure moved slightly forward then rearward again. It

may be noted that the Mach number corresponding to the most rearward location of the center of pressure for a given angle of attack increased with increase in angle of attack. For example, at an angle of attack of  $4^\circ$  the most rearward location of the center of pressure was at a Mach number of 0.94; whereas at an angle of attack of  $20^\circ$  the location occurred at a Mach number of 1.02. Figure 18 also shows that, for the Mach number and angle-of-attack ranges investigated, the center of pressure was always located ahead of the position of the quarter chord of the mean aerodynamic chord. The quarter chord of the mean aerodynamic chord was located at the 60-percent point of the fuselage length. The maximum rearward shift in the location of the fuselage center of pressure with increase in Mach number occurred at an angle of attack of  $4^\circ$  and was approximately 4 percent of the fuselage length, which is about 22 percent of the mean aerodynamic chord.

### CONCLUSIONS

From the aerodynamic loading investigation of a wing-fuselage combination having a wing of  $45^\circ$  sweepback at transonic speeds in the slotted test section of the Langley 8-foot transonic tunnel, the following conclusions are drawn:

1. In general, the aerodynamic characteristics of the wing-fuselage combination investigated in the slotted-throat test section at Mach numbers from 0.94 to 1.13 continue without discontinuity the trends with Mach numbers from 0.60 to 0.96 and at 1.2 indicated by the values obtained from the investigation of the same wing-fuselage combination in the closed-throat test section.
2. The spanwise loading on the wing at a constant angle of attack was characterized by outboard shifts in normal loading with increase in Mach number through the transonic speed range.
3. The loss in loading over the outboard sections of the wing which occurred with an increase in angle of attack and was due to separation was delayed to higher angles of attack with increase in Mach number through the transonic range. As a result, large increases in total load on the wing-fuselage combination were experienced with increase in Mach number through the transonic speed range, especially at the high angles of attack.
4. The chordwise center of pressure as well as the aerodynamic center of the wing shifted rearward with increase in Mach number through the transonic speed range.

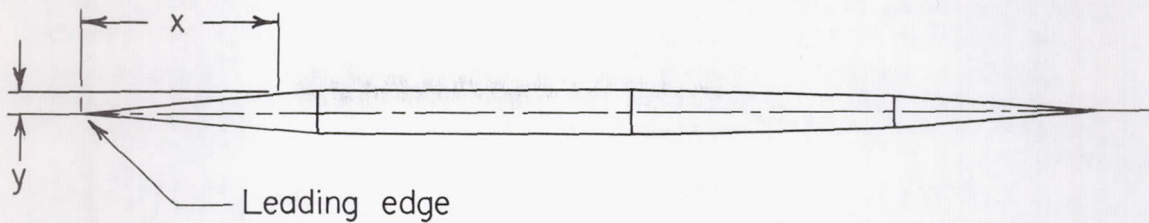
5. The percentage of total load carried by the fuselage decreased slightly through the transonic speed range. At the lower angles of attack the percentage of total load carried by the fuselage was approximately equal to the percentage of the total wing area blanketed by the fuselage, which was 16.5 percent. At the higher angles of attack the percentage of total load carried by the fuselage exceeded the percentage of the wing area blanketed by the fuselage. The peak values of the wing-induced loading on the fuselage decreased with increase in Mach number through the transonic speed range, but the influence of the wing on the loading spread rearward over the fuselage, and gave rise to a rearward shift in the center of pressure of the fuselage with increase in Mach number.

Langley Aeronautical Laboratory  
National Advisory Committee for Aeronautics  
Langley Field, Va.

#### REFERENCES

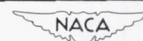
1. Loving, Donald L., and Williams, Claude V.: Basic Pressure Measurements on a Fuselage and a  $45^\circ$  Sweptback Wing-Fuselage Combination at Transonic Speeds in the Slotted Test Section of the Langley 8-Foot High-Speed Tunnel. NACA RM L51F05, 1951.
2. Loving, Donald L., and Estabrooks, Bruce B.: Transonic-Wing Investigation in the Langley 8-Foot High-Speed Tunnel at High Subsonic Mach Numbers and at a Mach Number of 1.2. Analysis of Pressure Distribution of Wing-Fuselage Configuration Having a Wing of  $45^\circ$  Sweepback, Aspect Ratio 4, Taper Ratio 0.6, and NACA 65A006 Airfoil Section. NACA RM L51F07, 1951.
3. Osborne, Robert S.: A Transonic-Wing Investigation in the Langley 8-Foot High-Speed Tunnel at High Subsonic Mach Numbers and at a Mach Number of 1.2. Wing-Fuselage Configuration Having a Wing of  $45^\circ$  Sweepback, Aspect Ratio 4, Taper Ratio 0.6, and NACA 65A006 Airfoil Section. NACA RM L50H08, 1950.
4. Wright, Ray H., and Ritchie, Virgil S.: Characteristics of a Transonic Test Section with Various Slot Shapes in the Langley 8-Foot High-Speed Tunnel. NACA RM L51H10, 1951.
5. Ritchie, Virgil S., and Pearson, Albin O.: Calibration of the Slotted Test Section of the Langley 8-Foot Transonic Tunnel and Preliminary Experimental Investigation of Boundary-Reflected Disturbances. NACA RM L51K14, 1951.

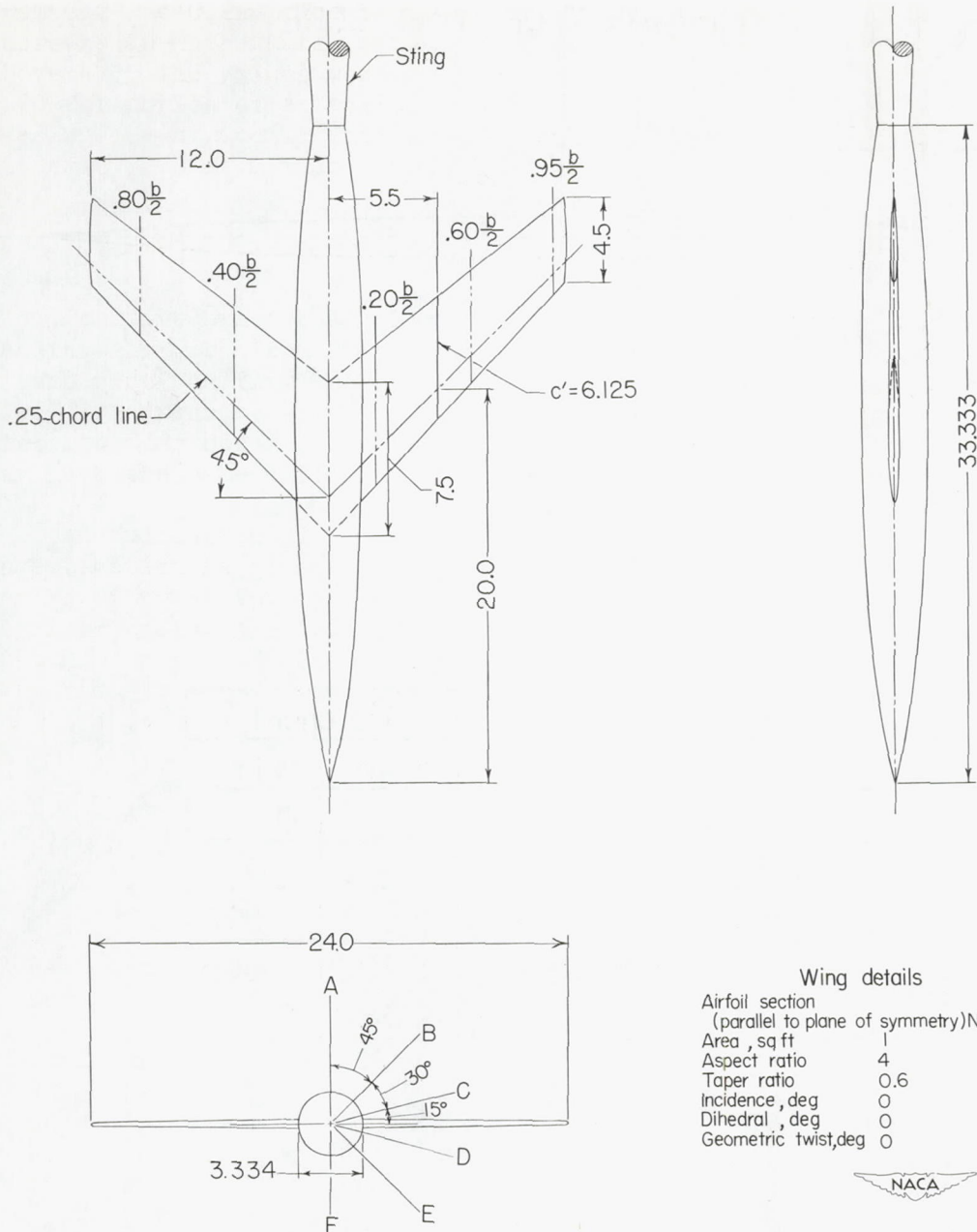
TABLE I  
COORDINATES OF WING CORE



Root chord	
x, in.	y, in.
0	0
1.688	.149
3.938	.149
5.813	.108
7.313	0

Tip chord	
x, in.	y, in.
0	0
1.013	.090
2.363	.090
3.488	.065
4.388	0





Wing details

Airfoil section	(parallel to plane of symmetry)NACA 65A006
Area , sq ft	1
Aspect ratio	4
Taper ratio	0.6
Incidence , deg	0
Dihedral , deg	0
Geometric twist,deg	0



Figure 1.- Details of the wing-fuselage combination investigated in the slotted test section of the Langley 8-foot transonic tunnel. (All dimensions are in inches except as otherwise noted.)

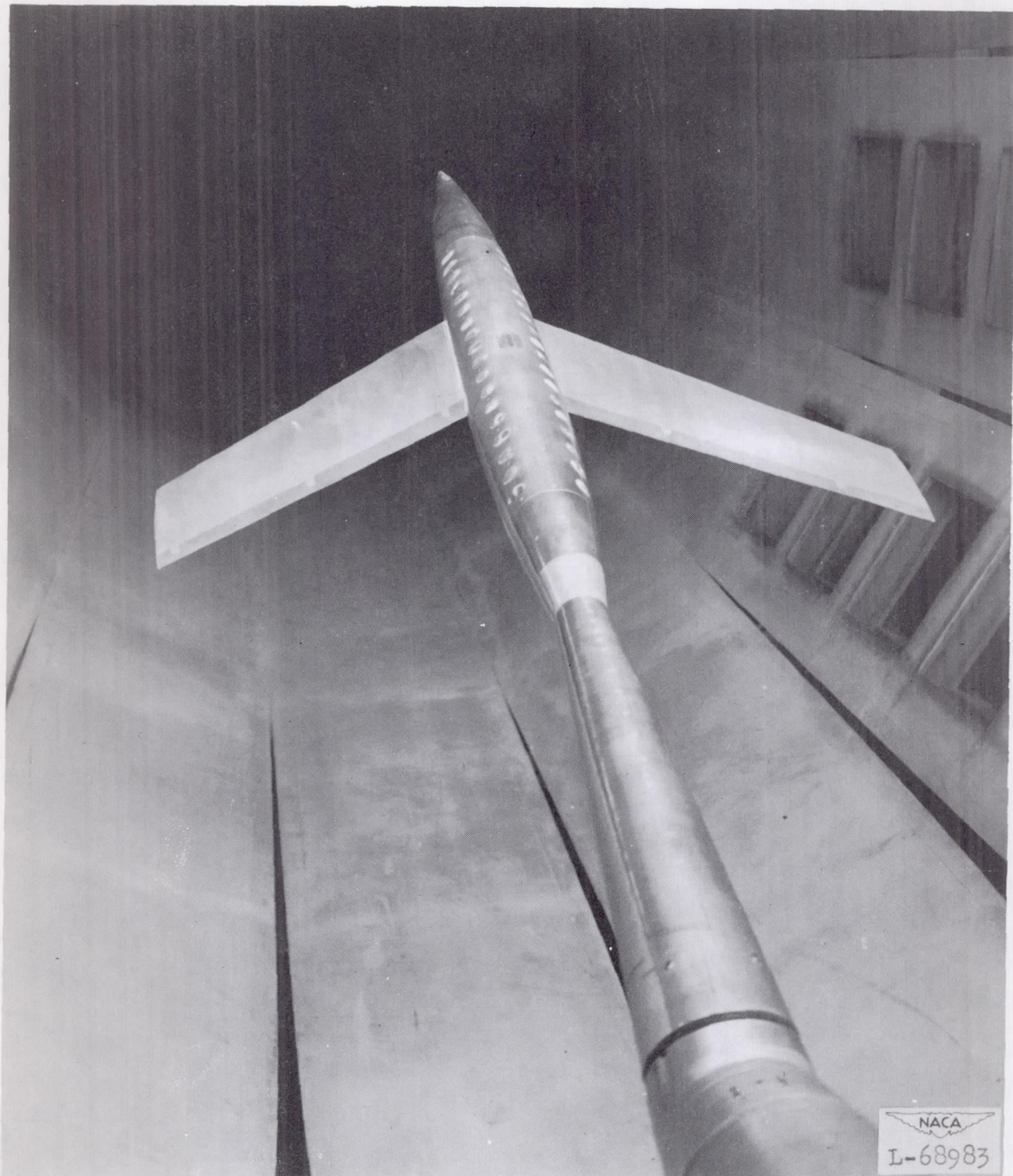


Figure 2.- Model installed in the slotted test section of the Langley 8-foot transonic tunnel.

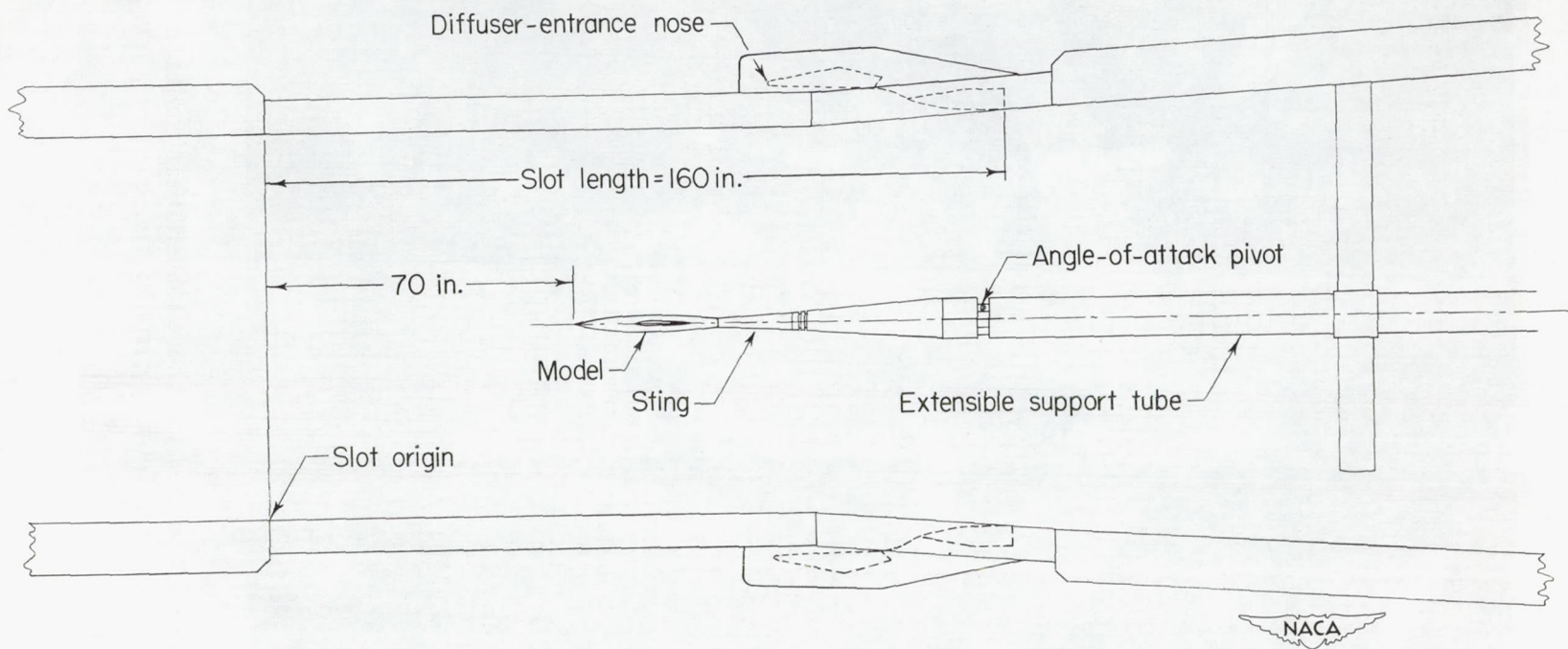


Figure 3.- Details of the location of the model in the slotted test section of the Langley 8-foot transonic tunnel.

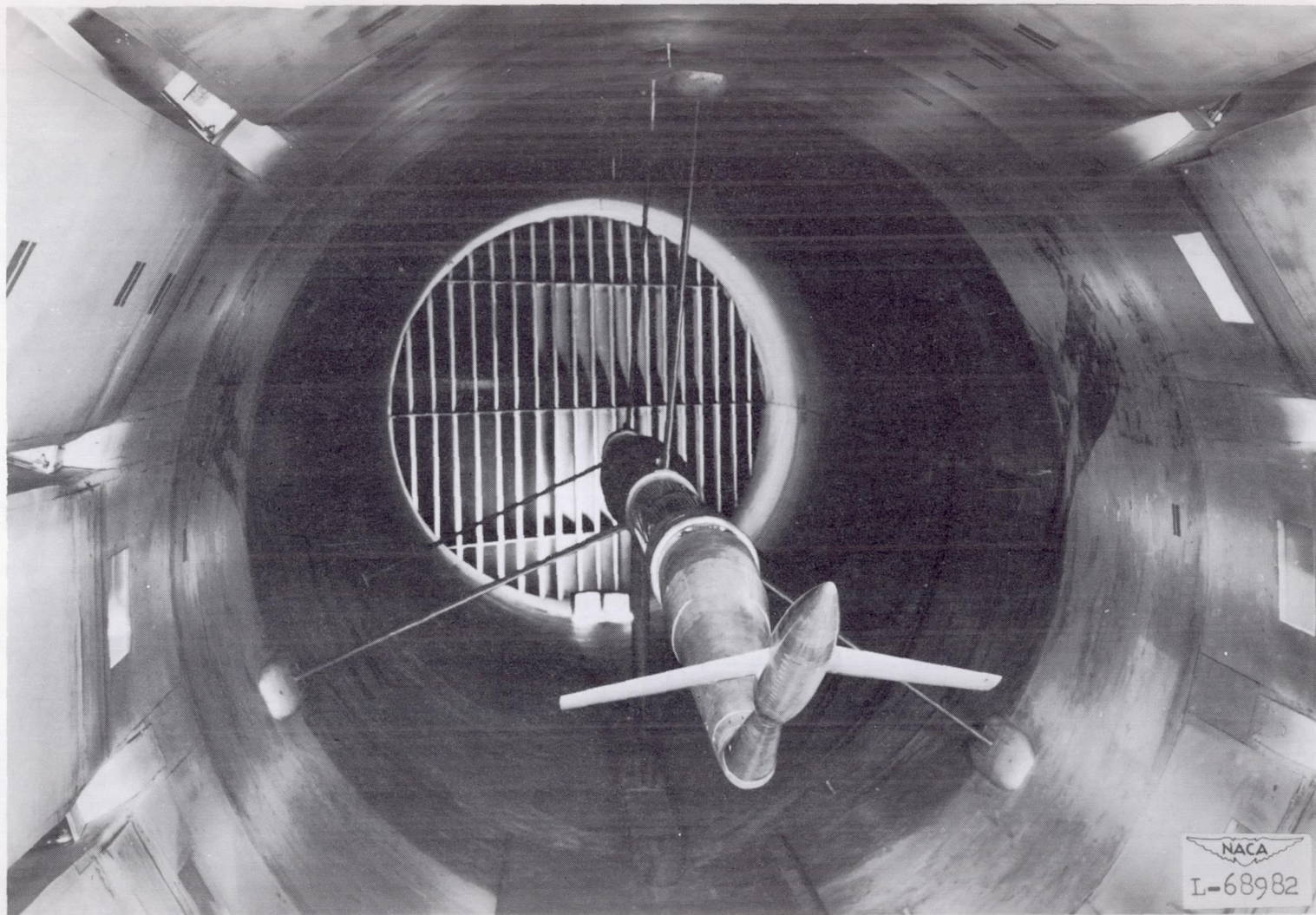


Figure 4.- Model support system for high angles of attack.

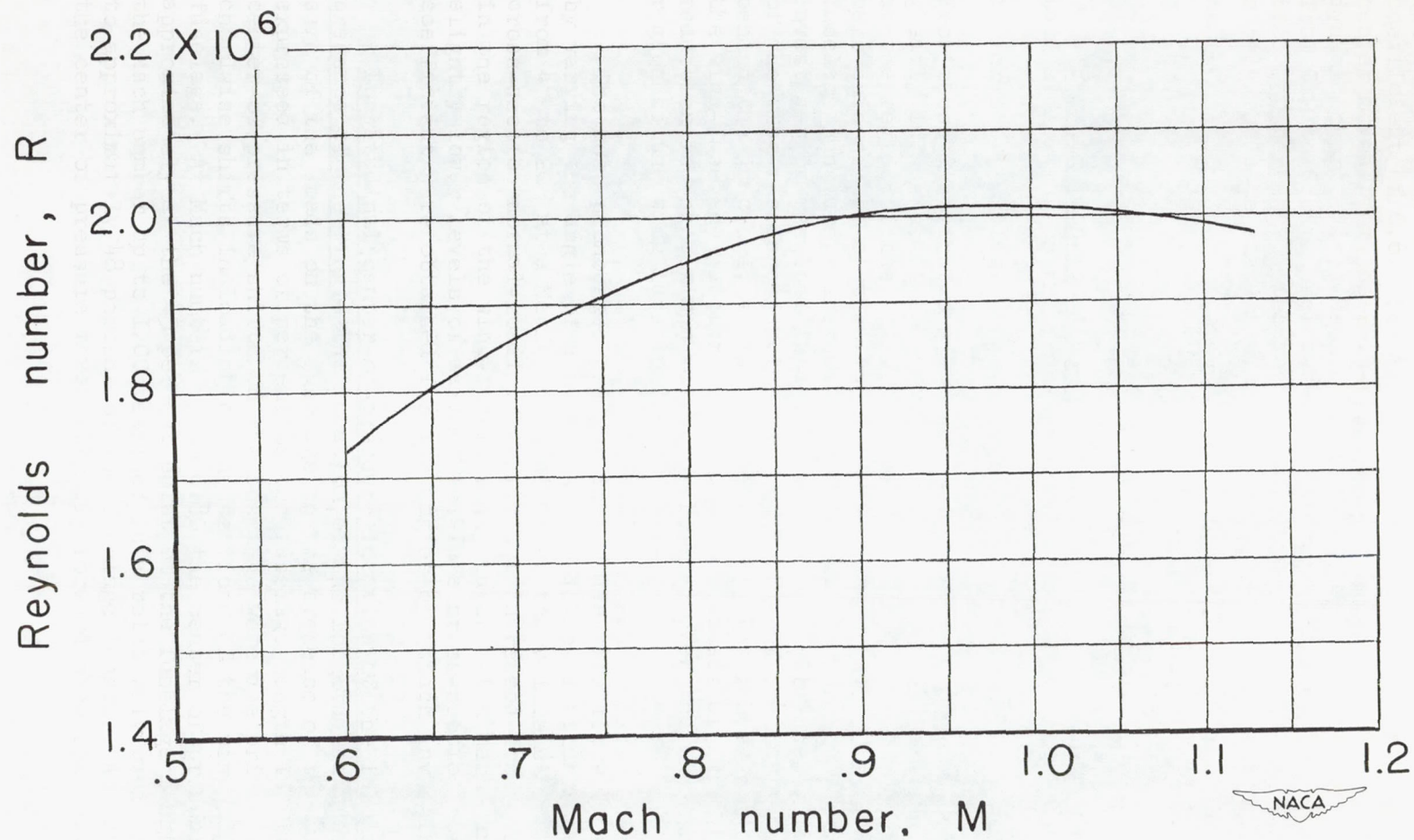
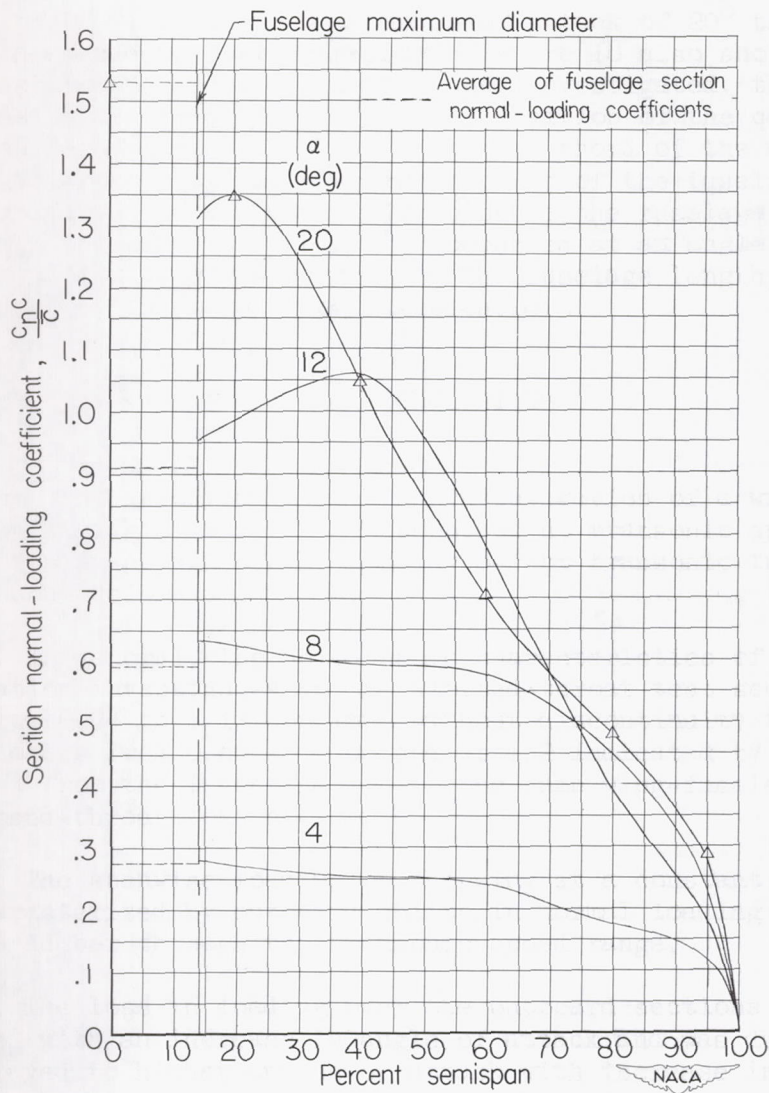
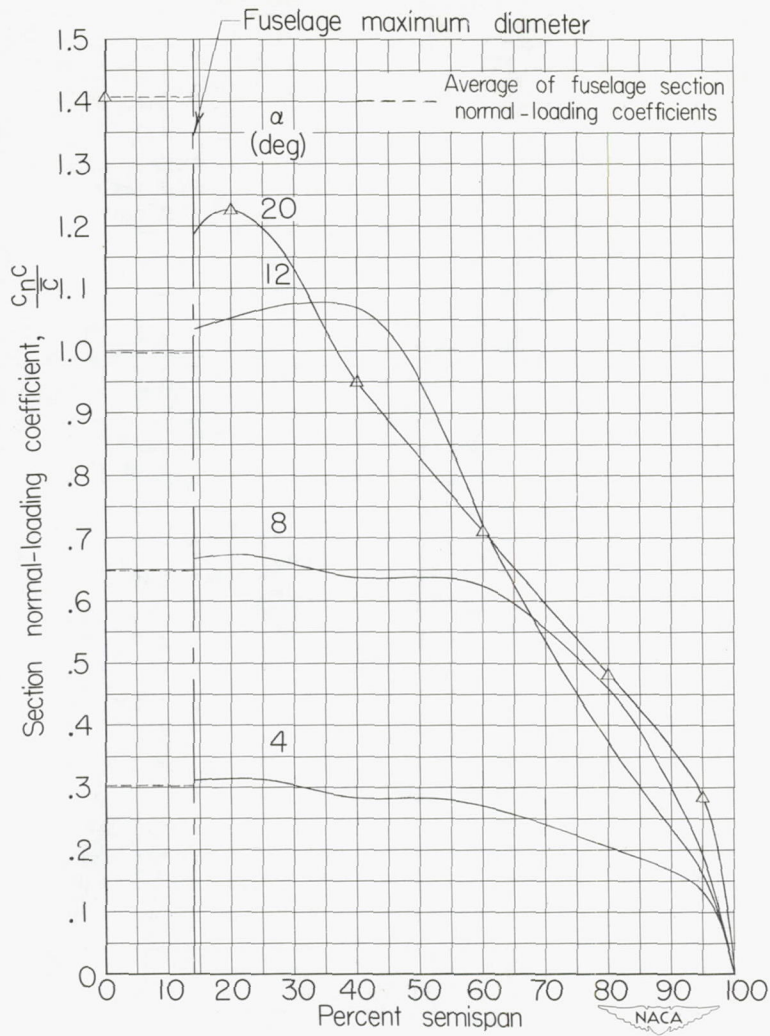


Figure 5.- Variation with Mach number of test Reynolds number based on a mean aerodynamic chord of 6.125 inches.



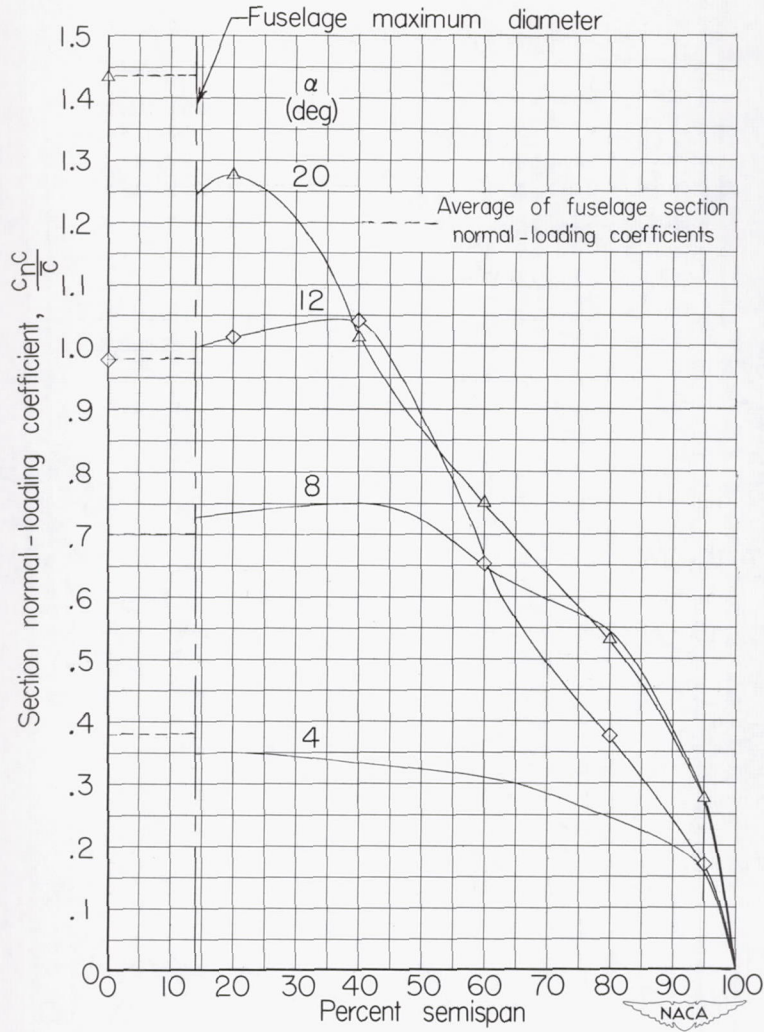
(a)  $M = 0.60$ .

Figure 6.- The spanwise distributions of section normal-loading coefficient at several angles of attack. (Lines without symbols indicate closed-throat data.)



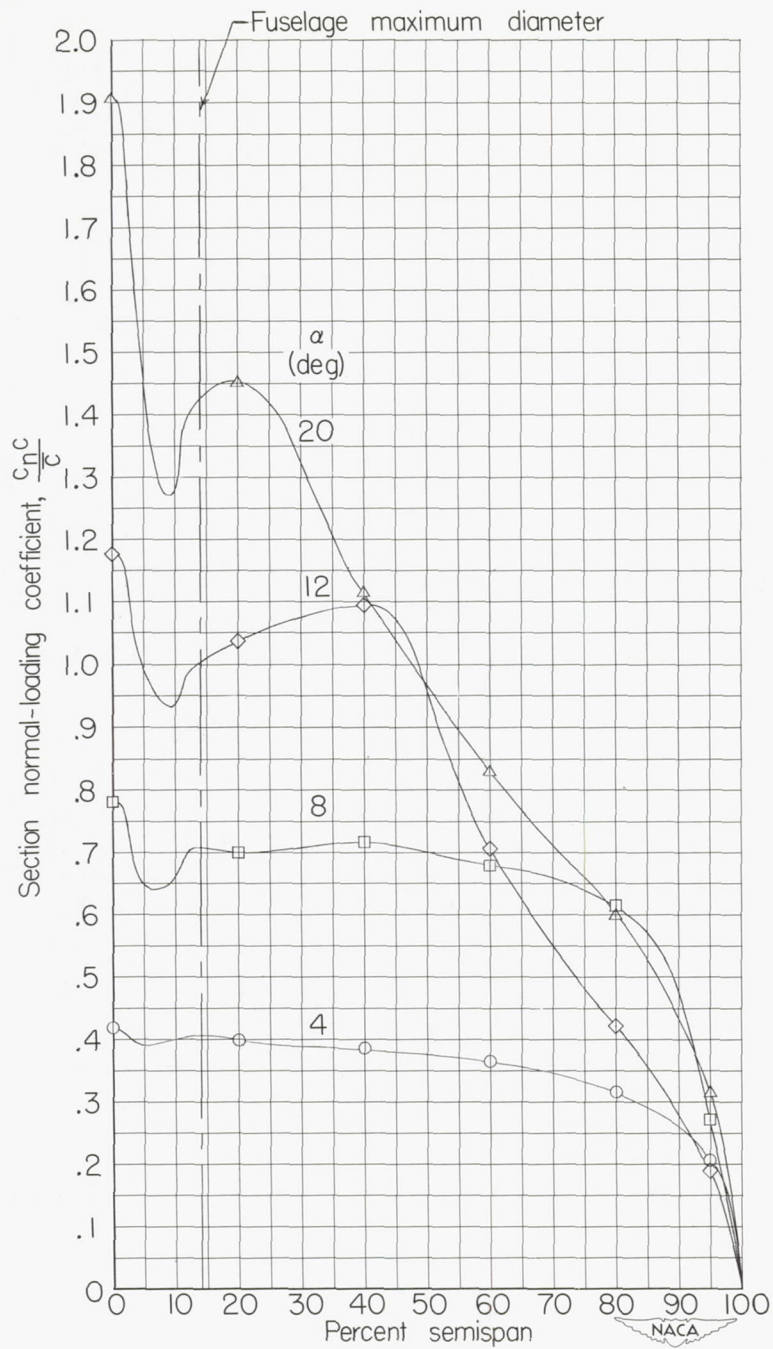
(b)  $M = 0.79$ , slotted-throat data;  $M = 0.80$ , closed-throat data.

Figure 6.- Continued.



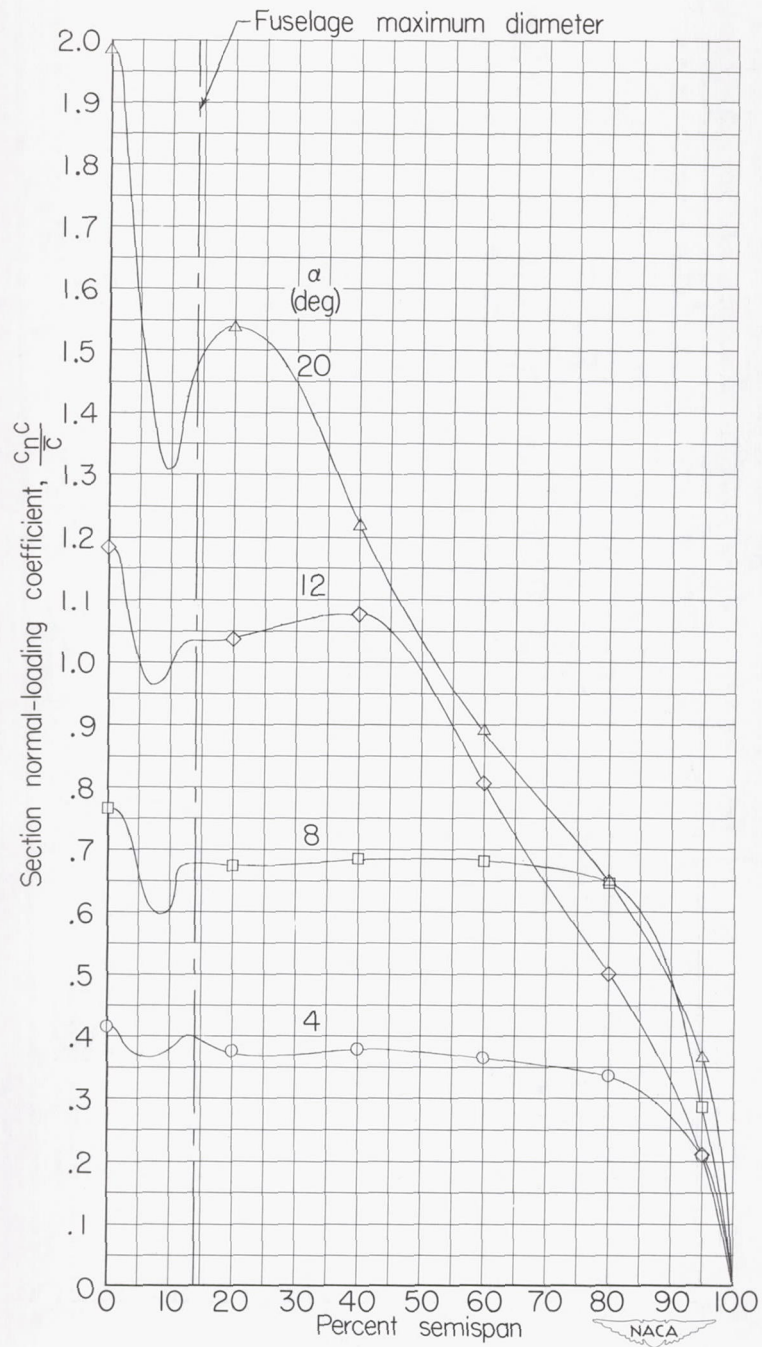
(c)  $M = 0.89$ , slotted-throat data;  $M = 0.90$ , closed-throat data.

Figure 6.- Continued.



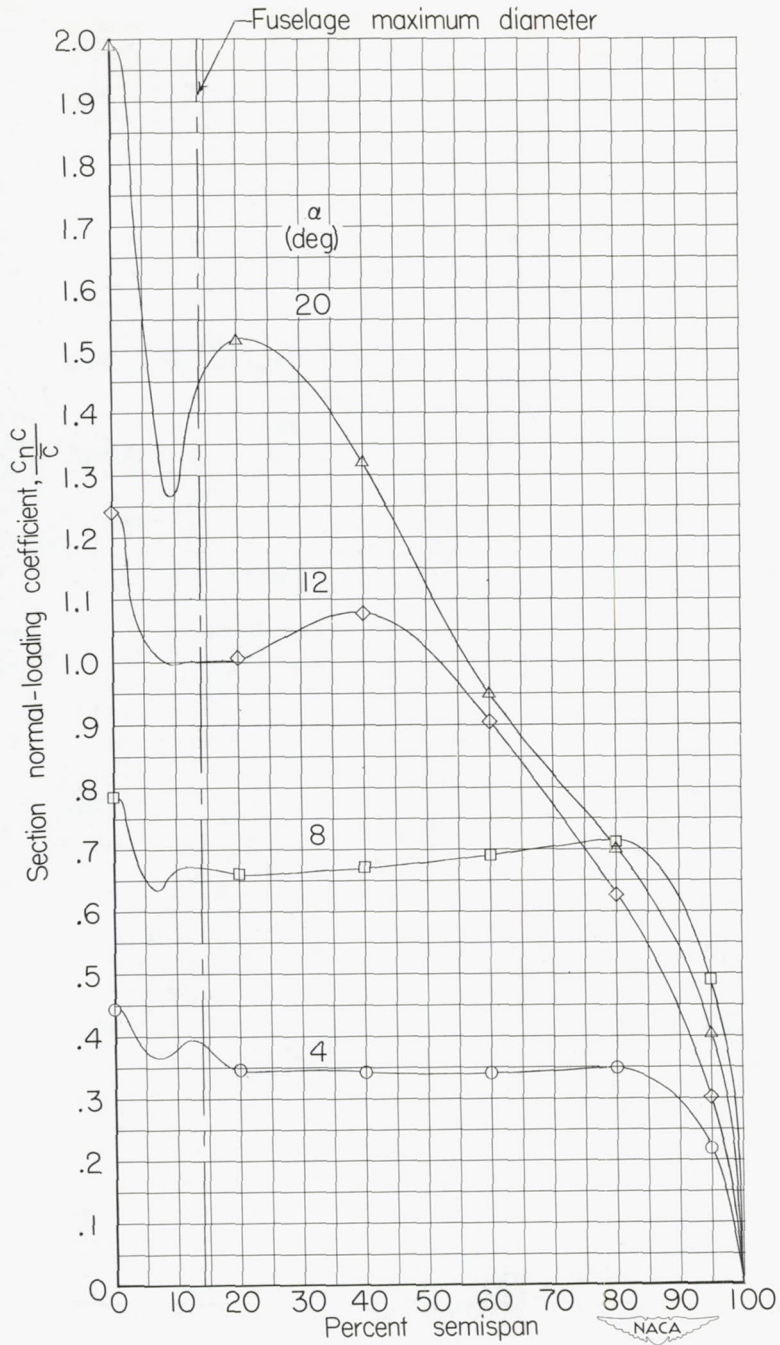
(d)  $M = 0.94$ .

Figure 6.- Continued.



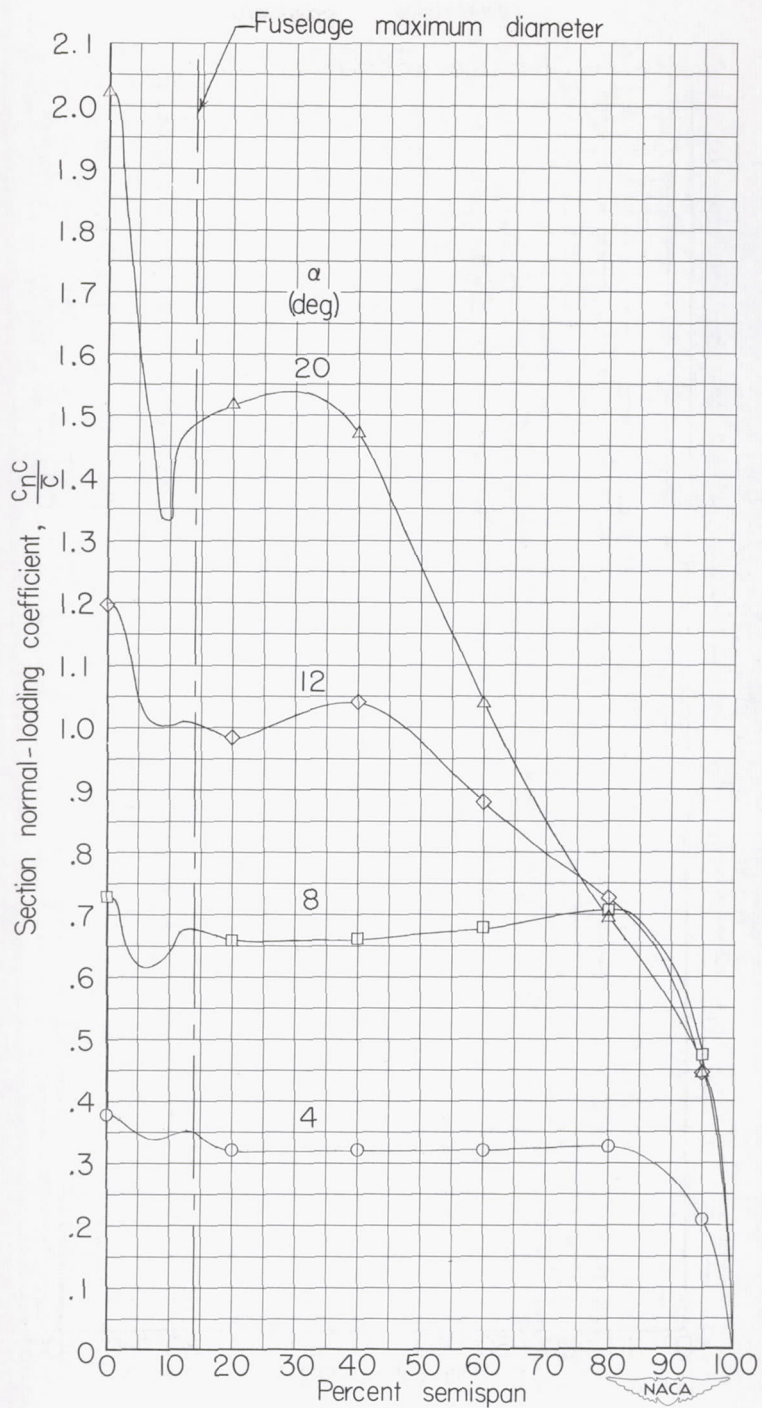
(e)  $M = 0.97$ .

Figure 6.- Continued.



(f)  $M = 0.99$ .

Figure 6.- Continued.



(g)  $M = 1.02$ .

Figure 6.- Continued.

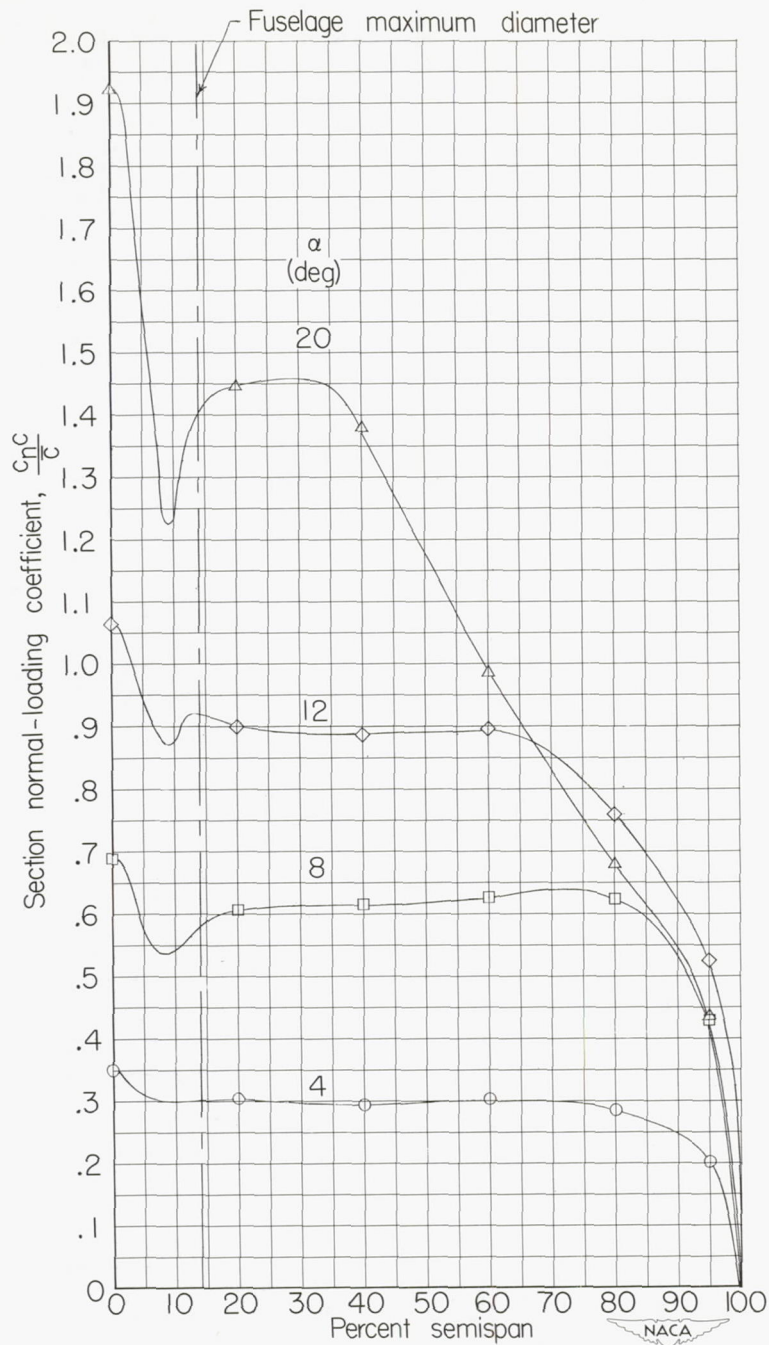
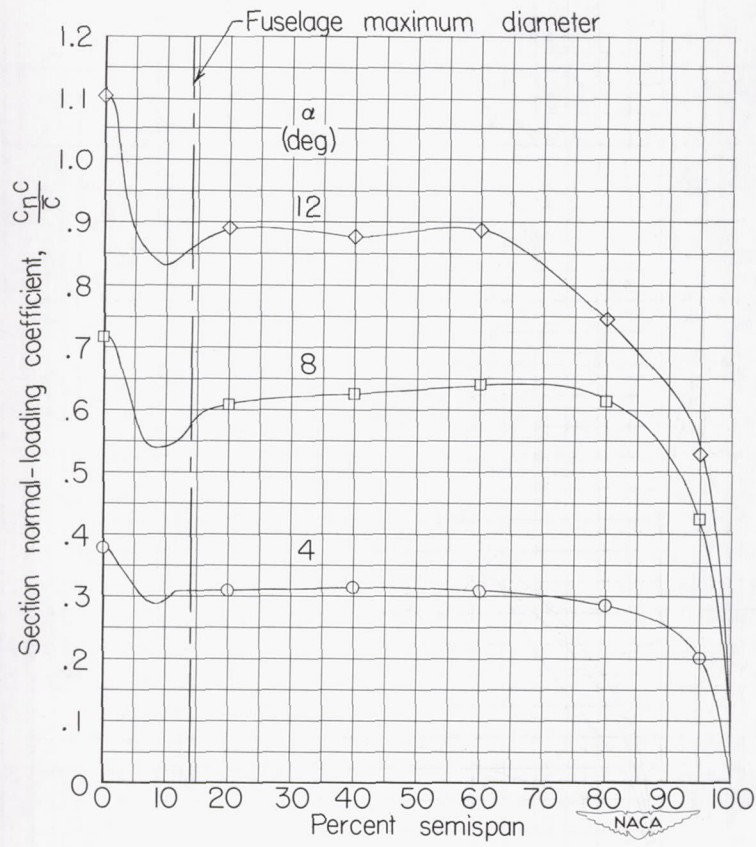
(h)  $M = 1.11$ .

Figure 6.- Continued.



(i)  $M = 1.13$ .

Figure 6.- Concluded.

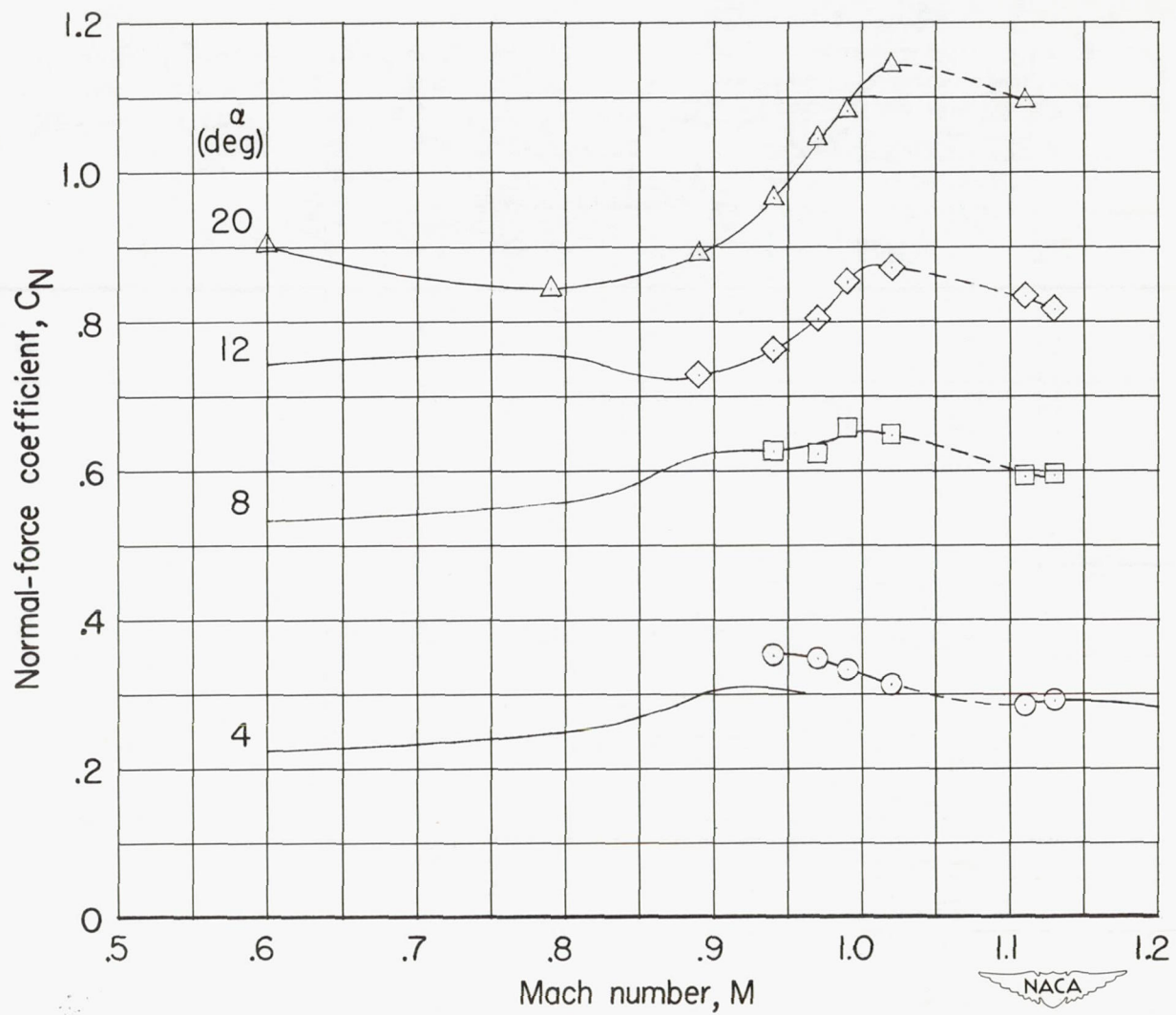


Figure 7.- The variation with Mach number of the normal-force coefficient of the wing-fuselage combination at several angles of attack.

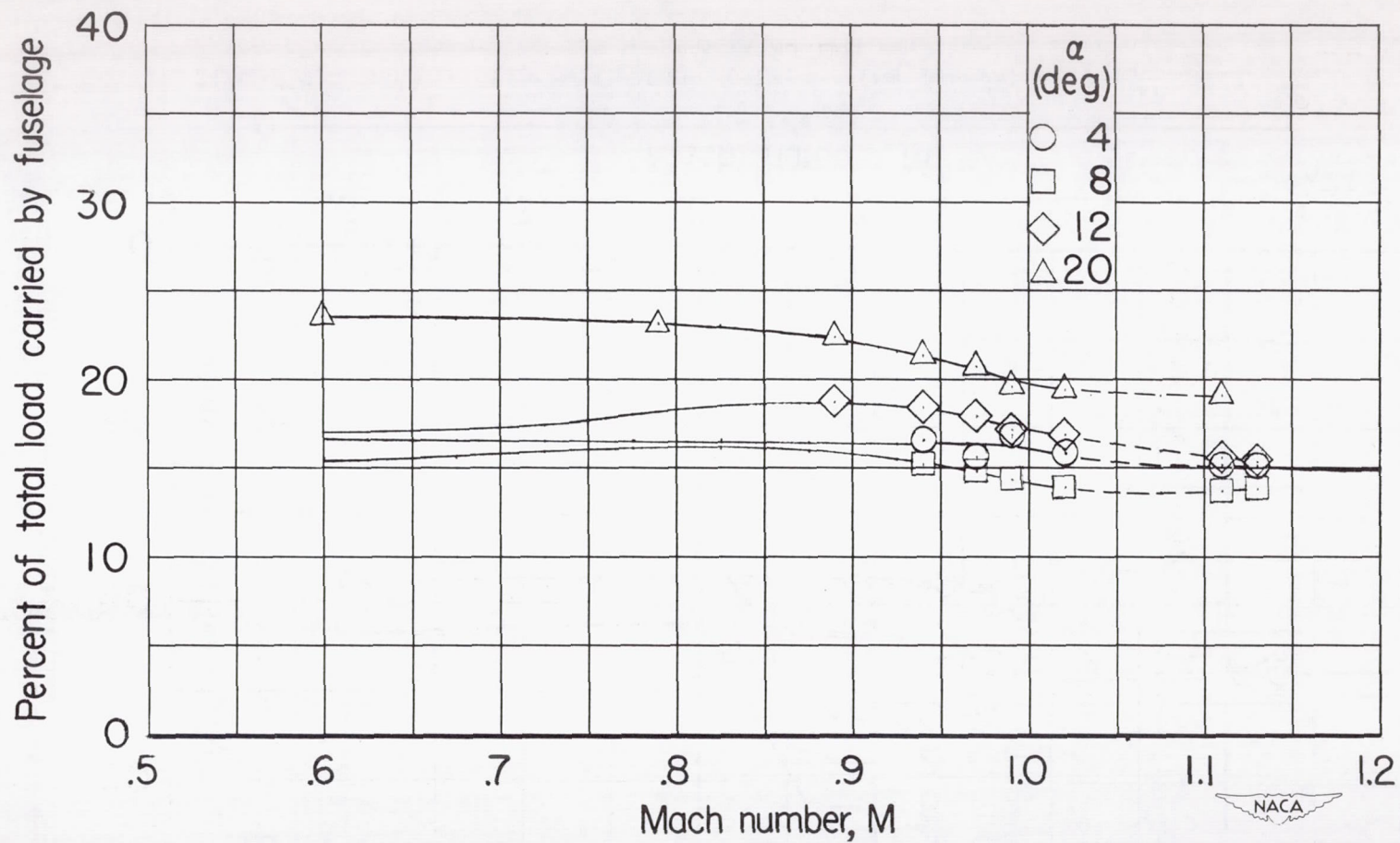


Figure 8.- The variation with Mach number of the load carried by the fuselage relative to the load on the wing-fuselage combination at several angles of attack.

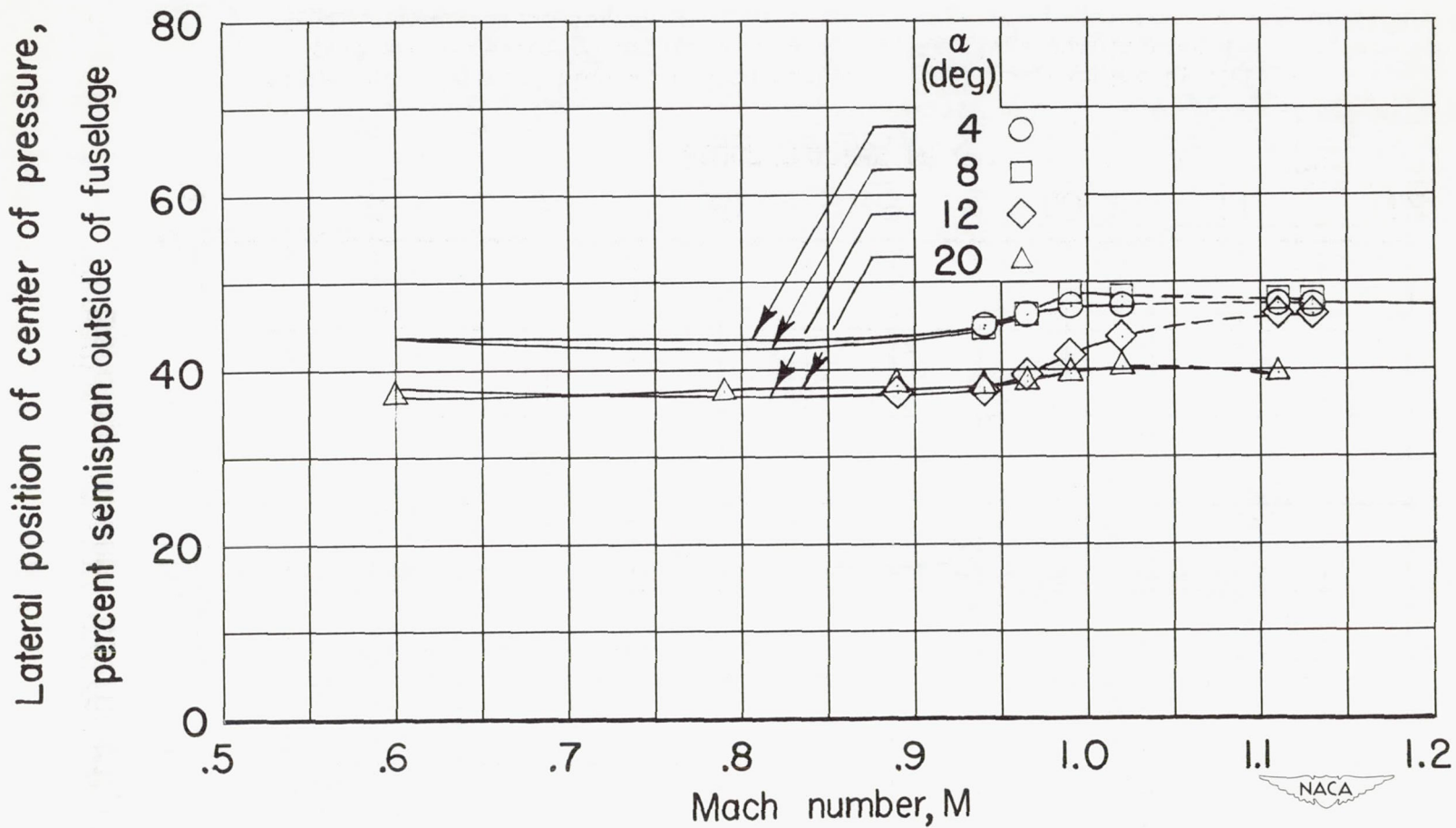


Figure 9.- The variation with Mach number of the lateral position of center of pressure of the wing outside the fuselage at several angles of attack.

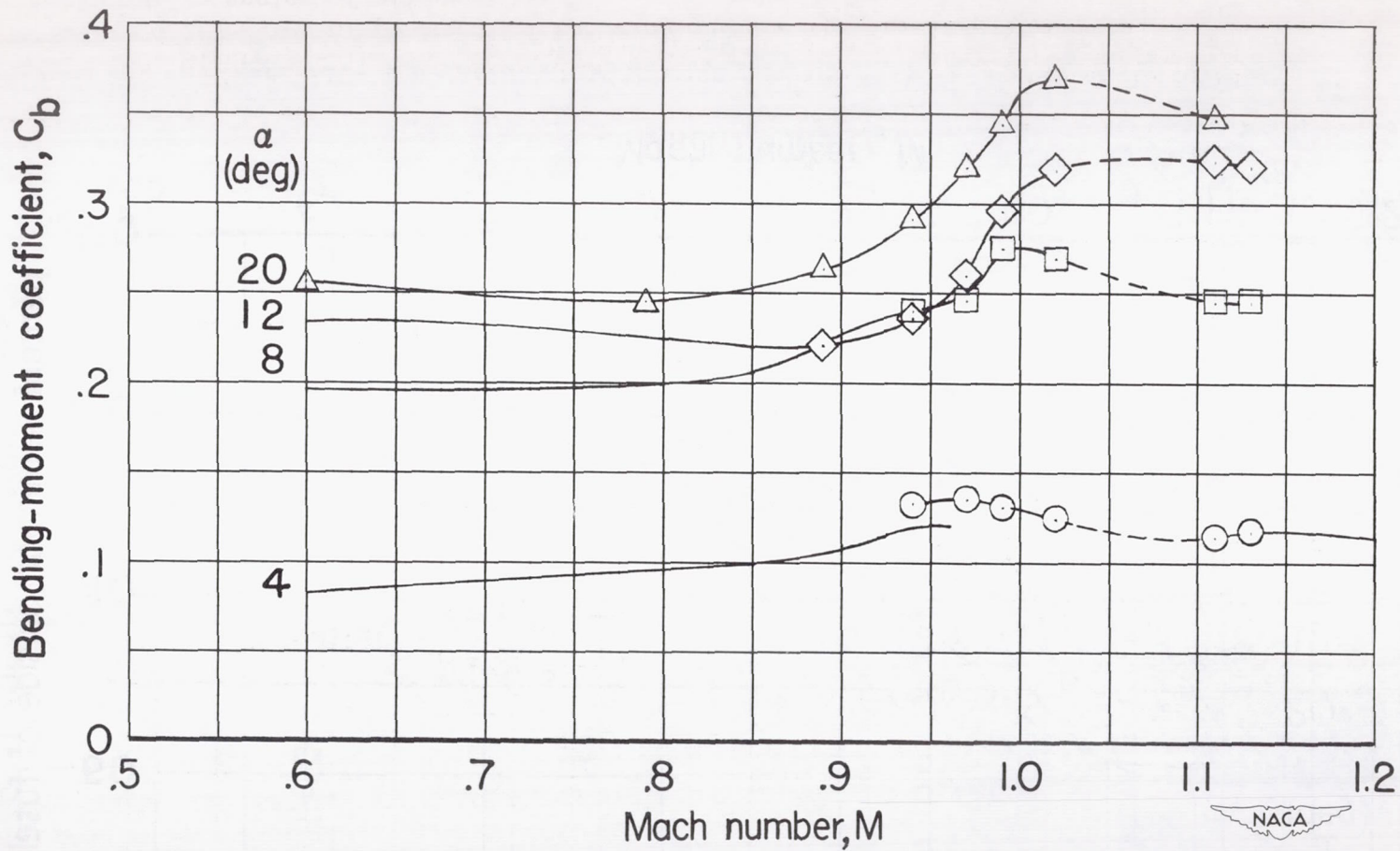


Figure 10.- The variation with Mach number of the bending-moment coefficient of the wing outside the fuselage about the wing-fuselage juncture at several angles of attack.



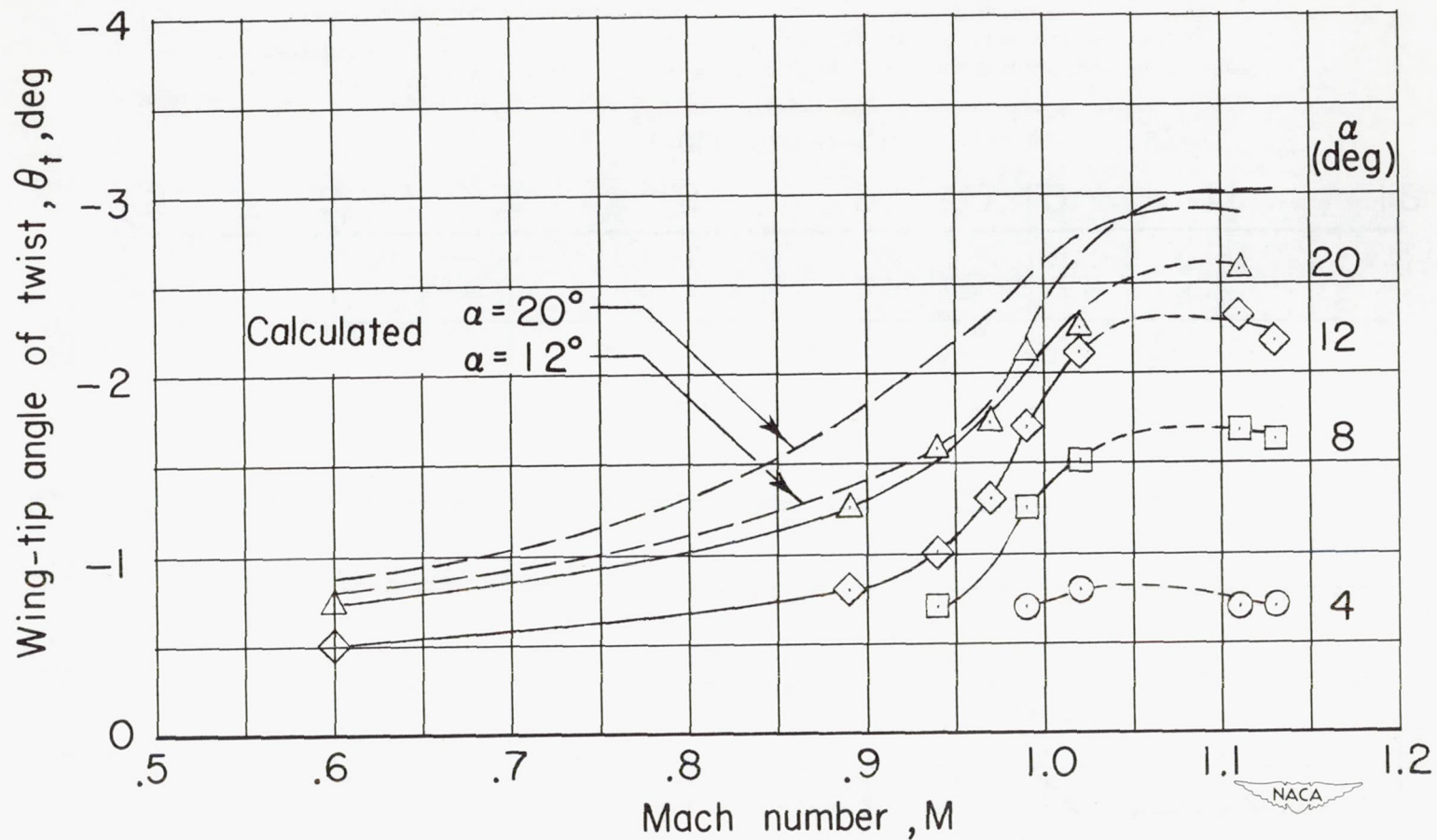
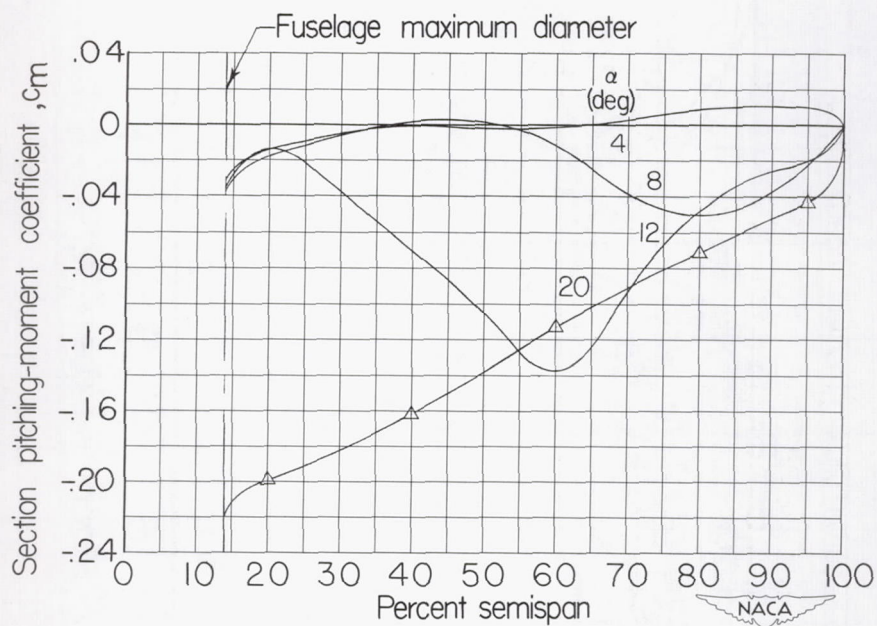
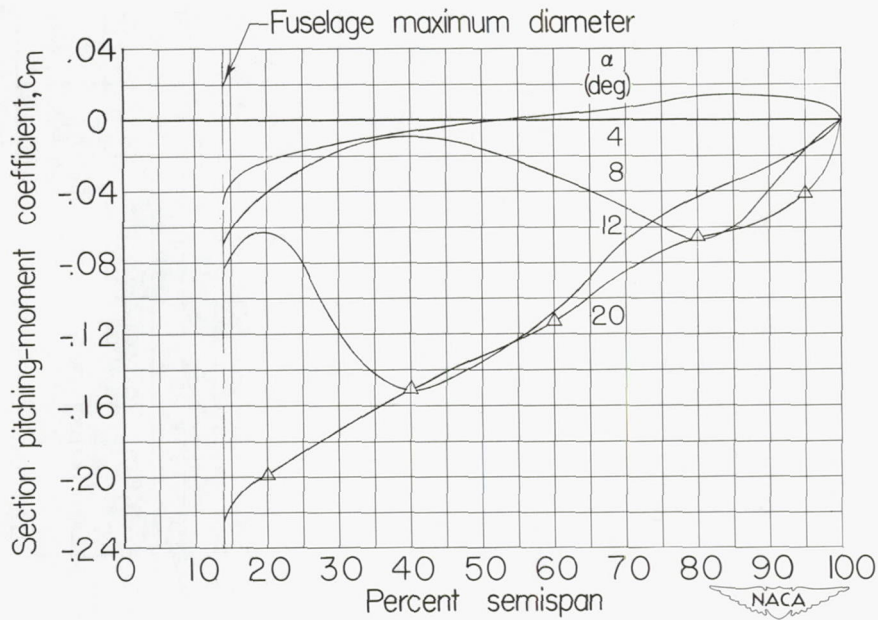


Figure 11.- The variation with Mach number of the wing-tip angle of twist at several angles of attack.



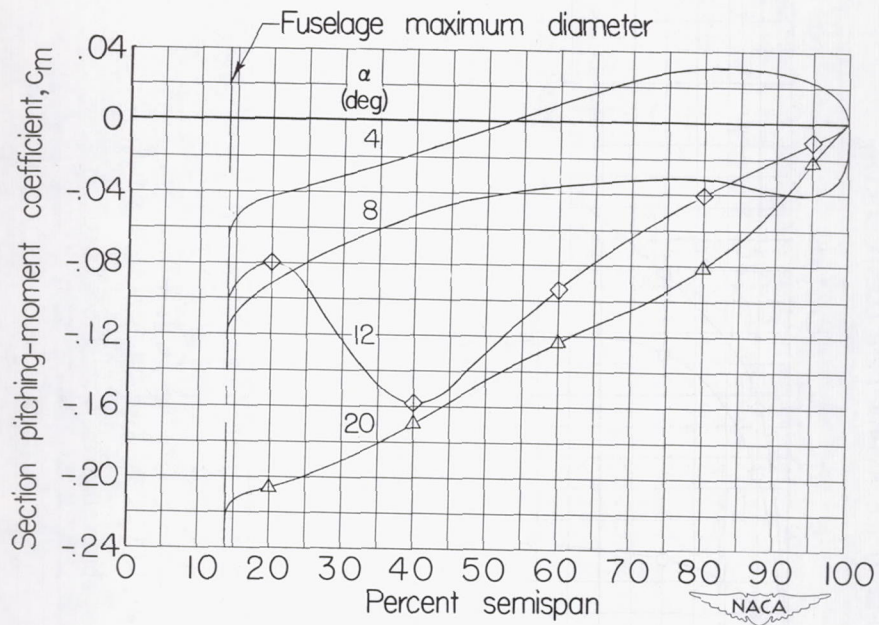
(a)  $M = 0.60$ .

Figure 12.- The spanwise distributions of section pitching-moment coefficient at several angles of attack.



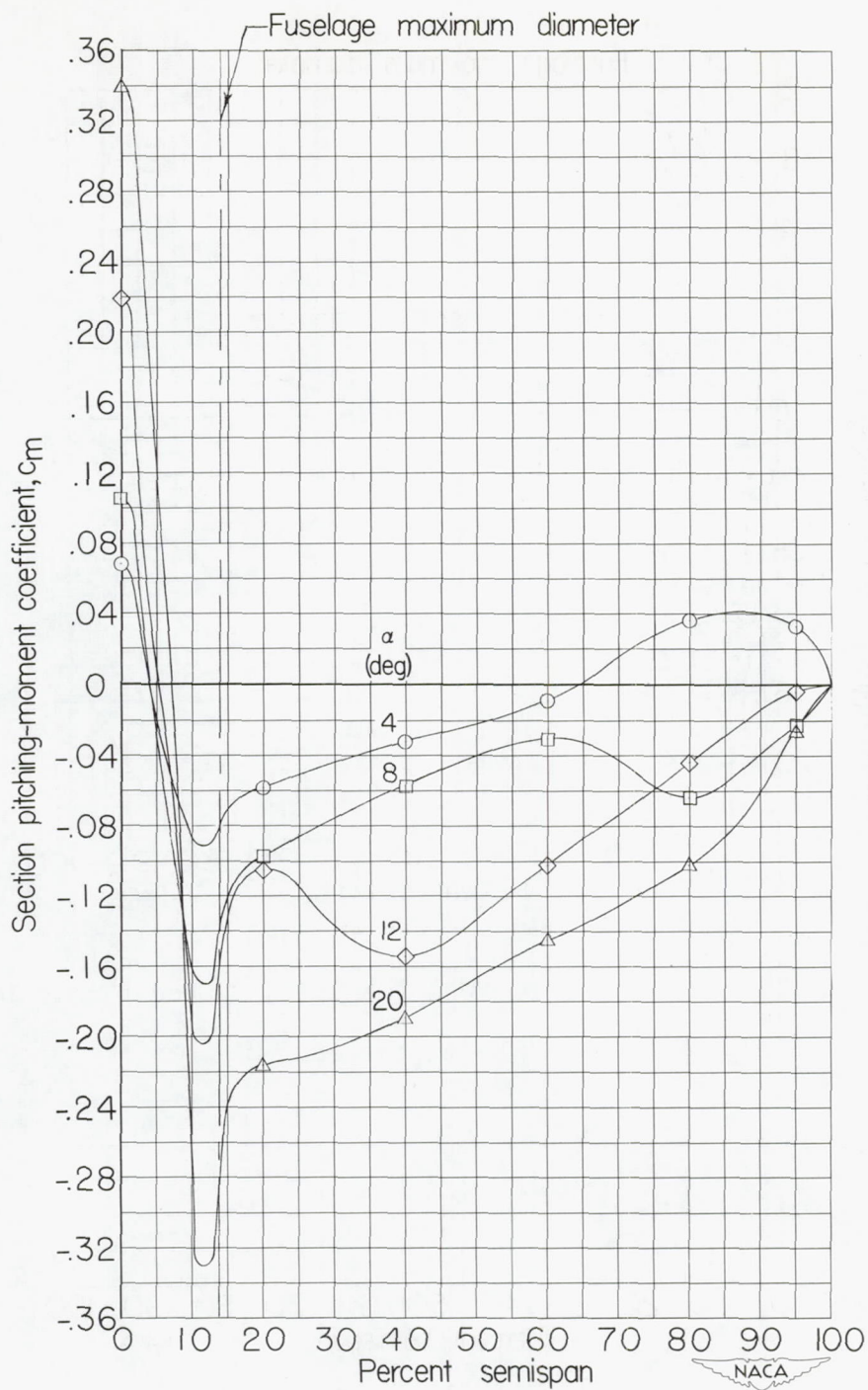
(b)  $M = 0.79$ , slotted-throat data;  $M = 0.80$ , closed-throat data.

Figure 12.- Continued.



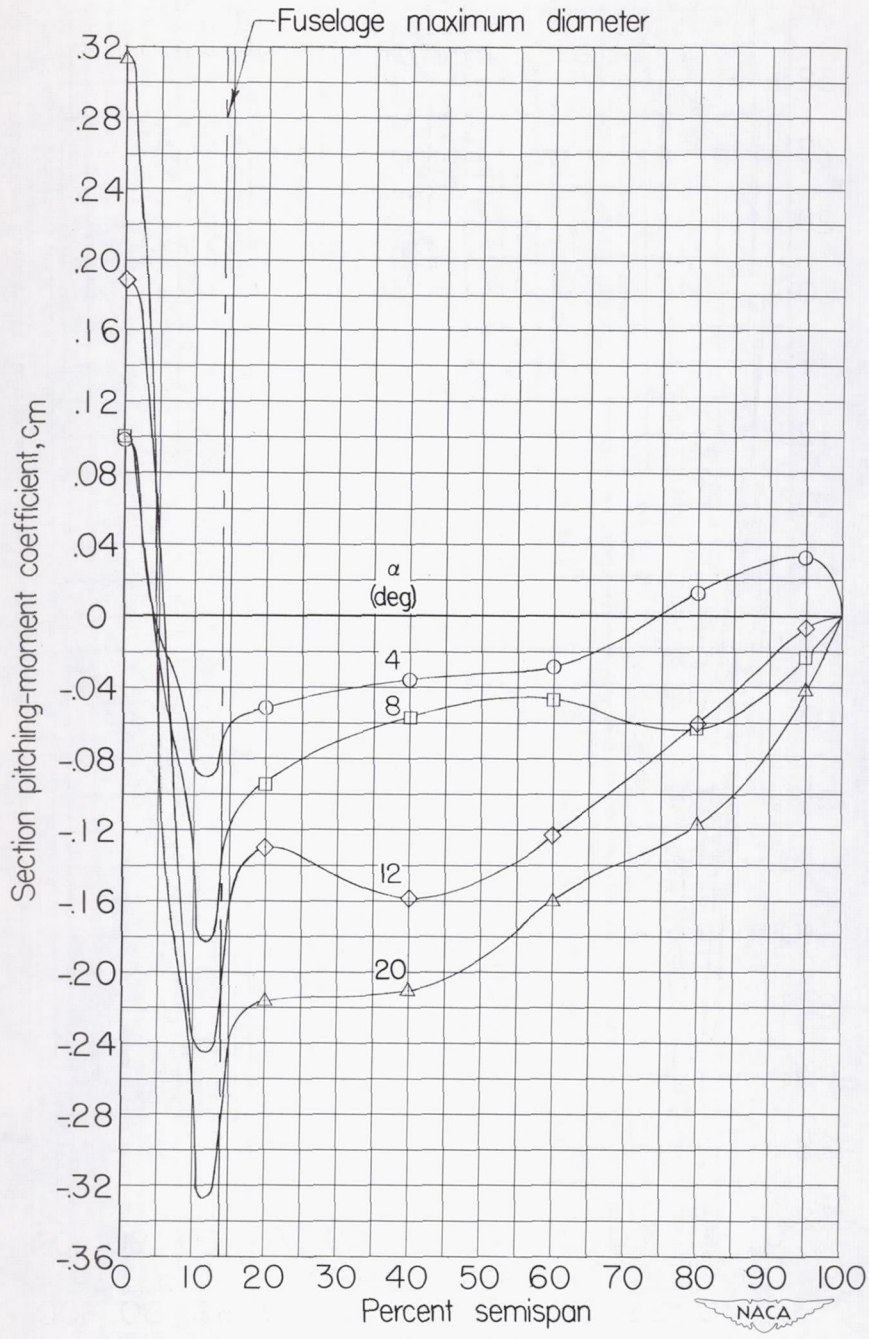
(c)  $M = 0.89$ , slotted-throat data;  $M = 0.90$ , closed-throat data.

Figure 12.- Continued.



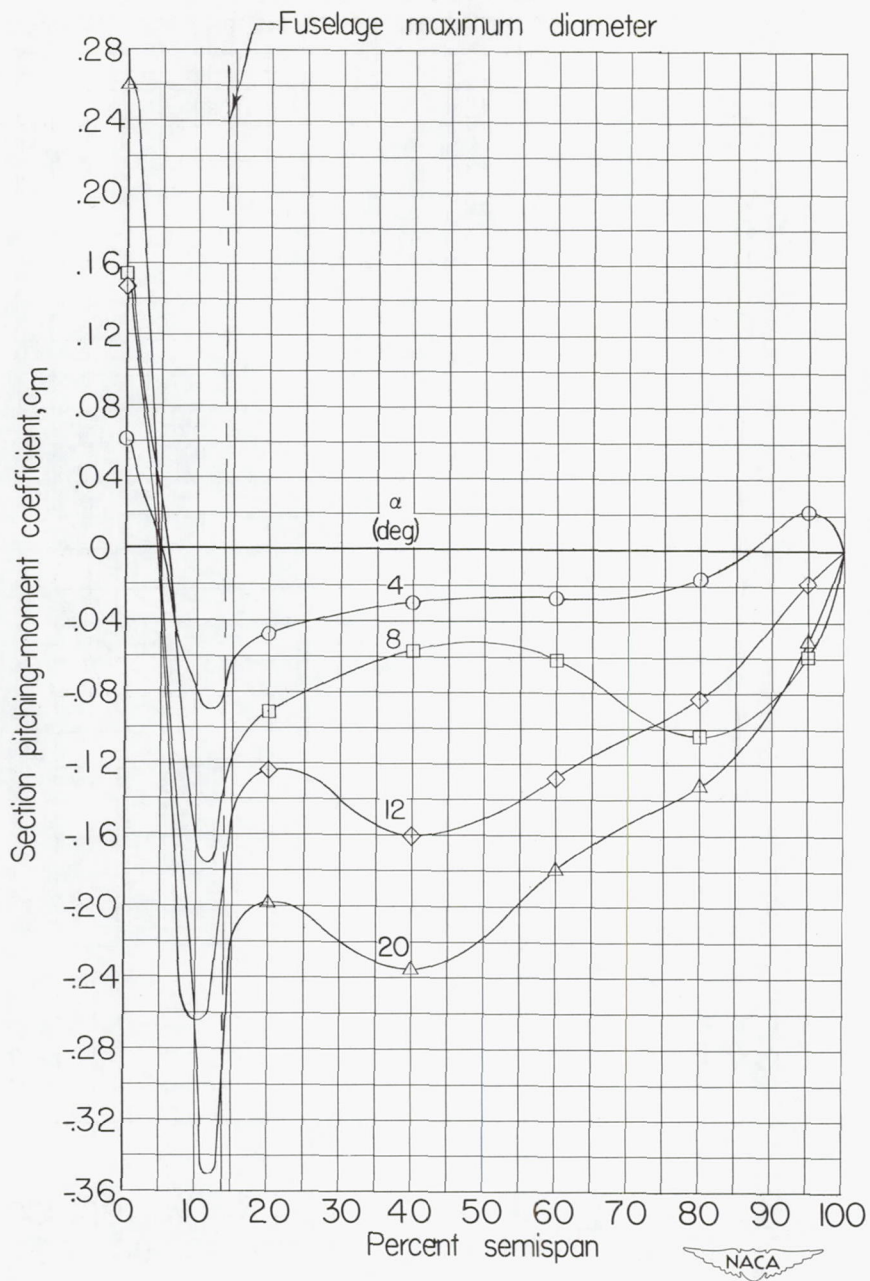
(d)  $M = 0.94$ .

Figure 12.- Continued.



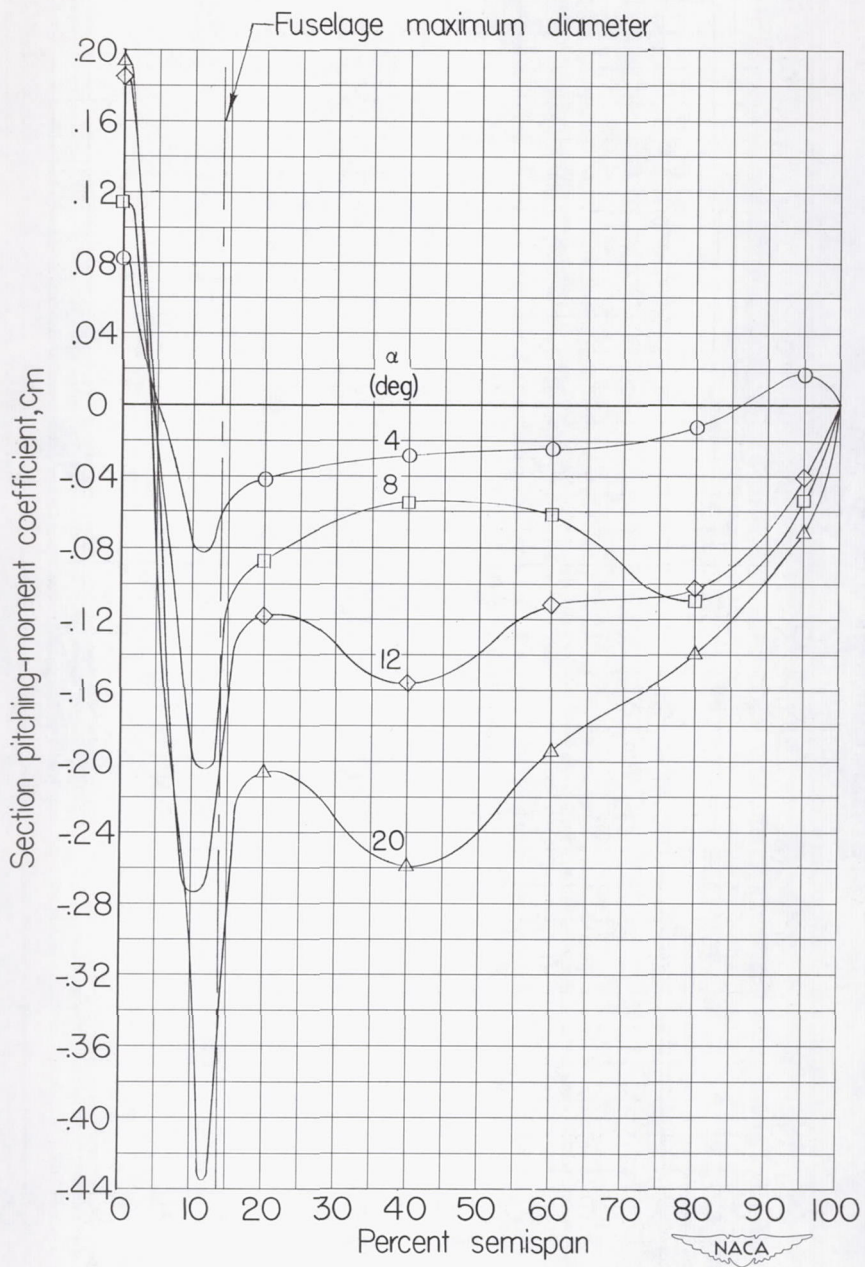
(e)  $M = 0.97$ .

Figure 12.- Continued.



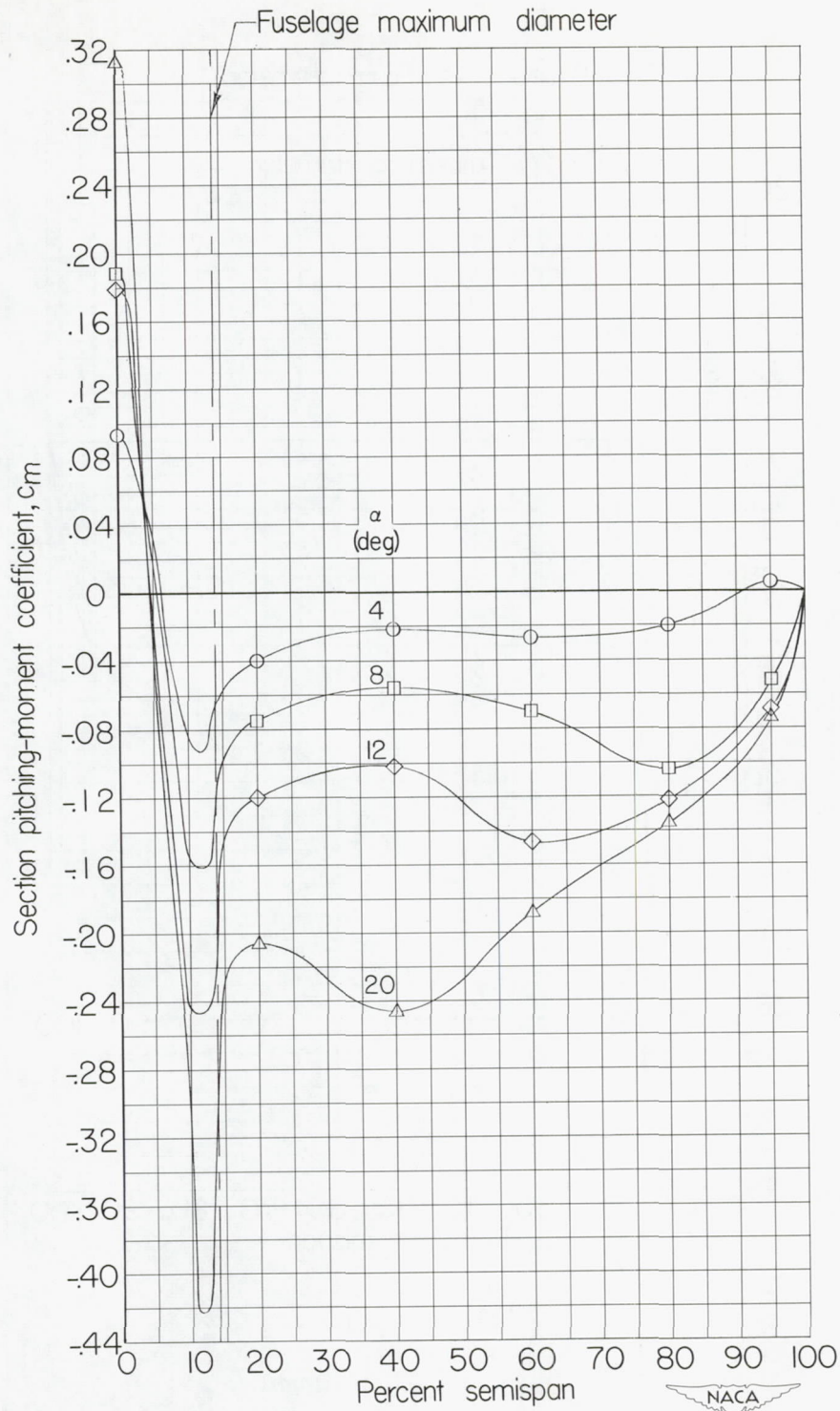
(f)  $M = 0.99$ .

Figure 12.- Continued.



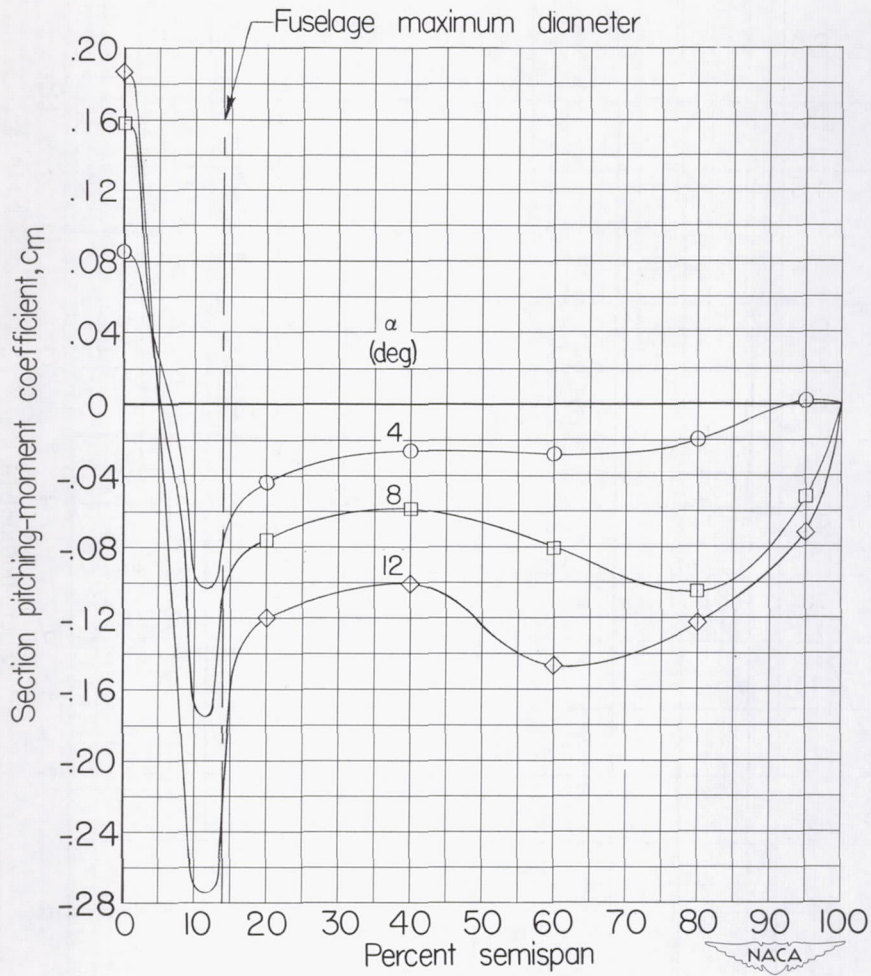
(g)  $M = 1.02$ .

Figure 12.- Continued.



(h)  $M = 1.11$ .

Figure 12.- Continued.



(i)  $M = 1.13$ .

Figure 12.- Concluded.

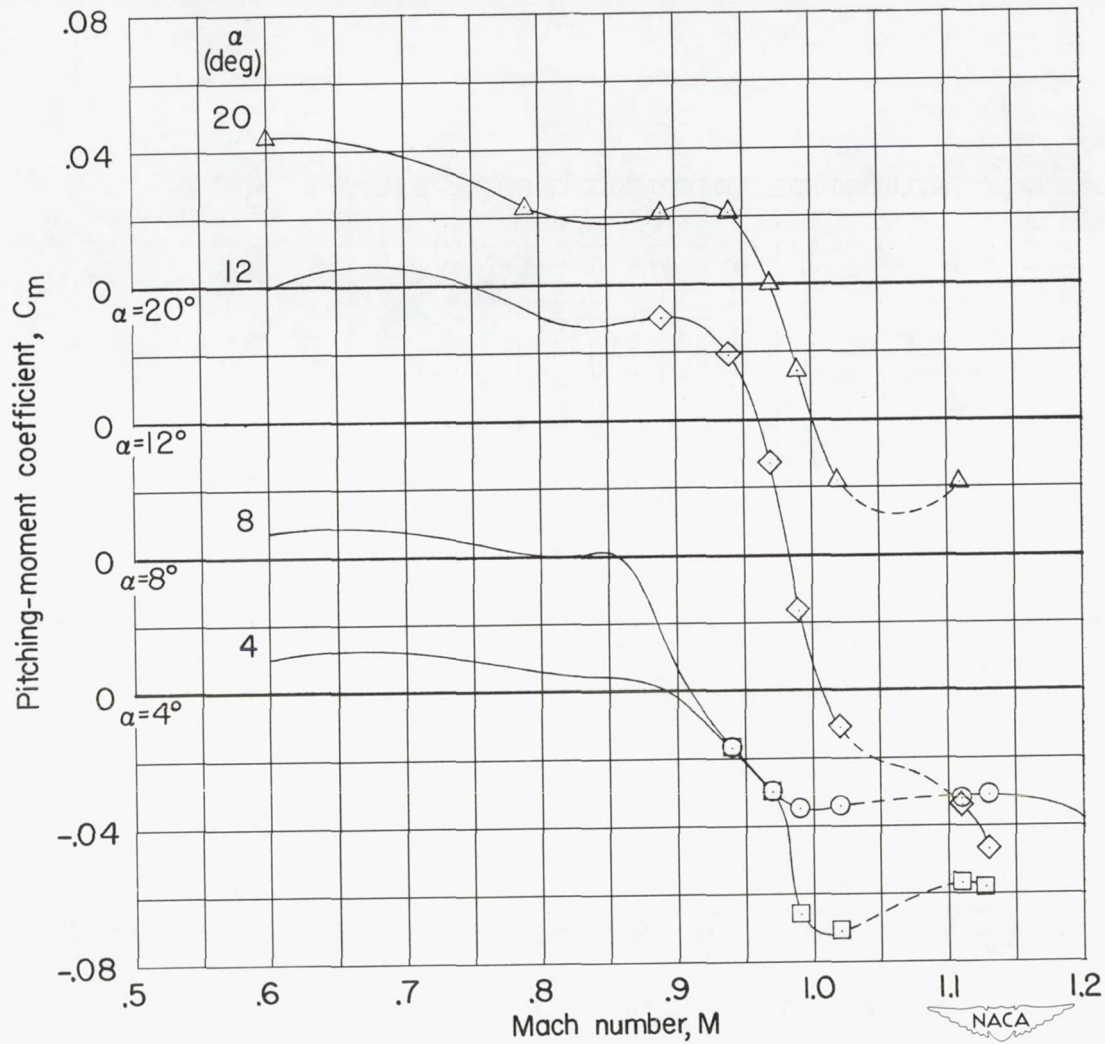


Figure 13.- The variation with Mach number of the pitching-moment coefficient of the wing-fuselage combination at several angles of attack.

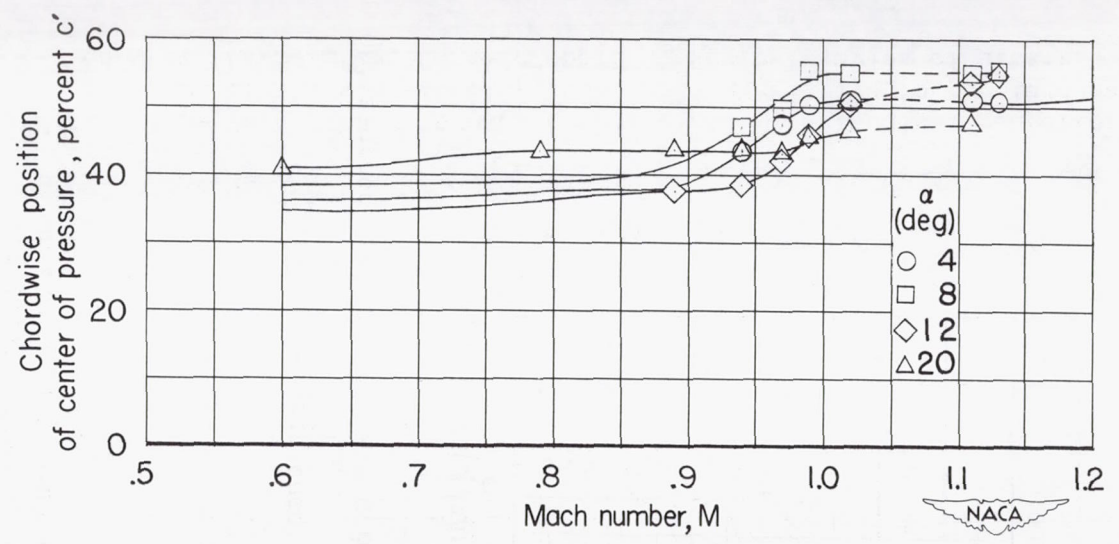


Figure 14.- The variation with Mach number of the chordwise center of pressure of the wing outside the fuselage relative to the leading edge of the mean aerodynamic chord at several angles of attack.

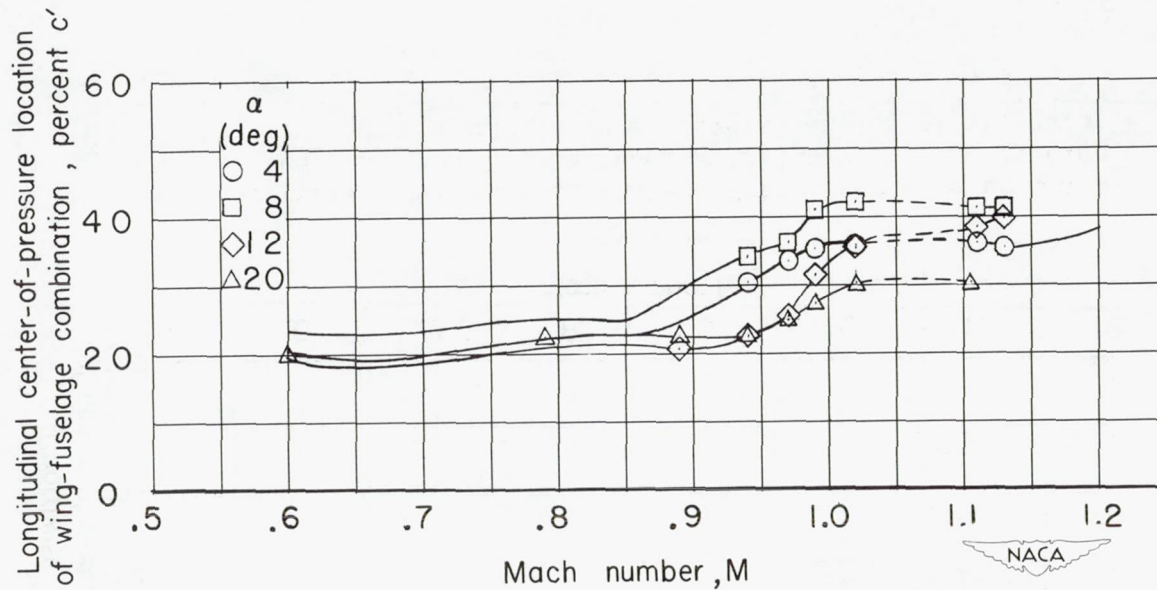


Figure 15.- Variation with Mach number of the longitudinal center of pressure of the wing-fuselage combination relative to the leading edge of the mean aerodynamic chord at several angles of attack.

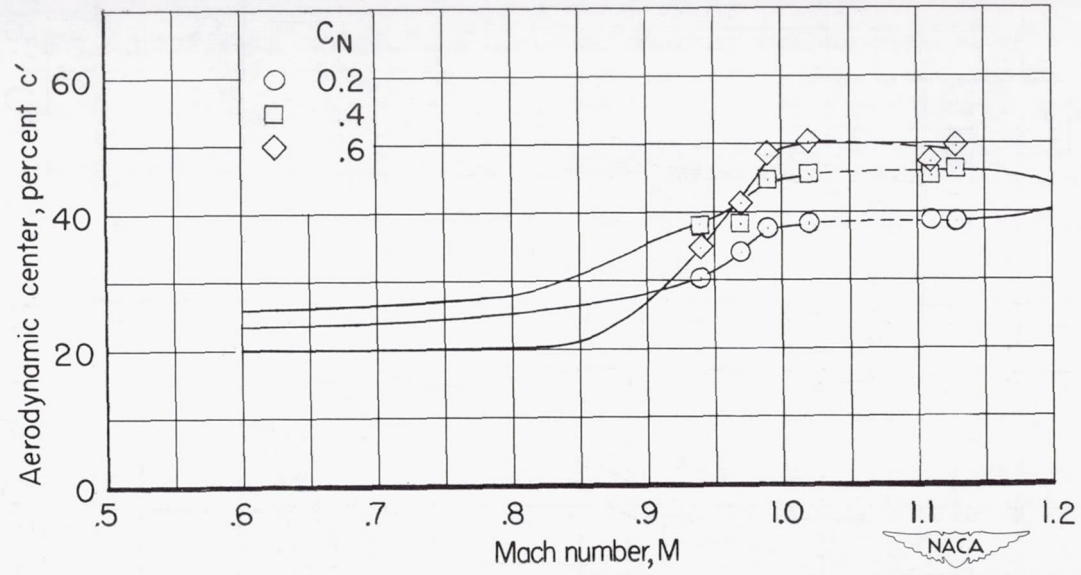
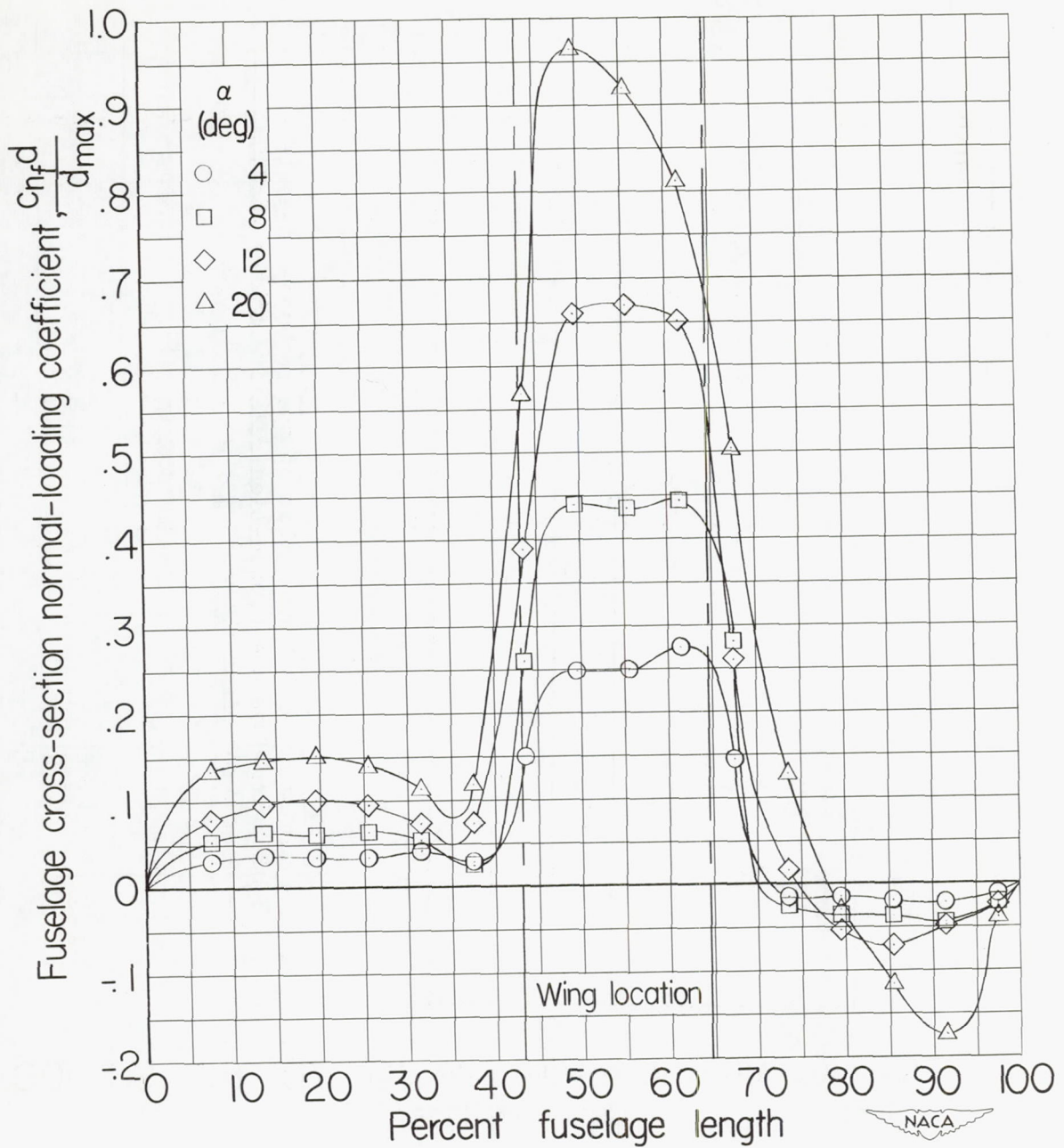
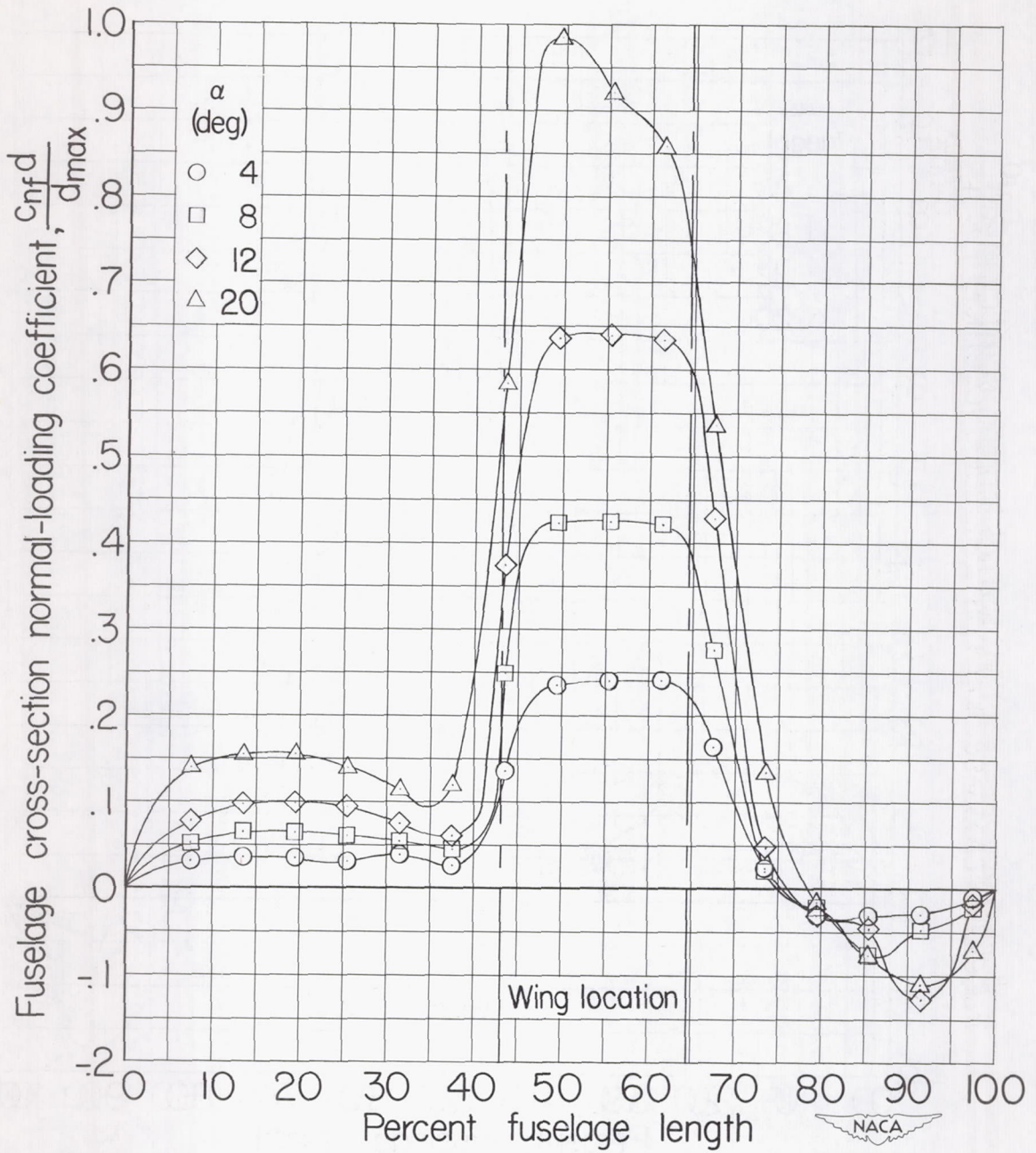


Figure 16.- The variation with Mach number of the aerodynamic-center location of the wing-fuselage combination relative to the leading edge of the mean aerodynamic chord.  $C_N = 0.2, 0.4, 0.6$ .



(a)  $M = 0.94$ .

Figure 17.- The longitudinal distribution of loading over the fuselage with wing present at several angles of attack.



(b)  $M = 0.97$ .

Figure 17.- Continued.

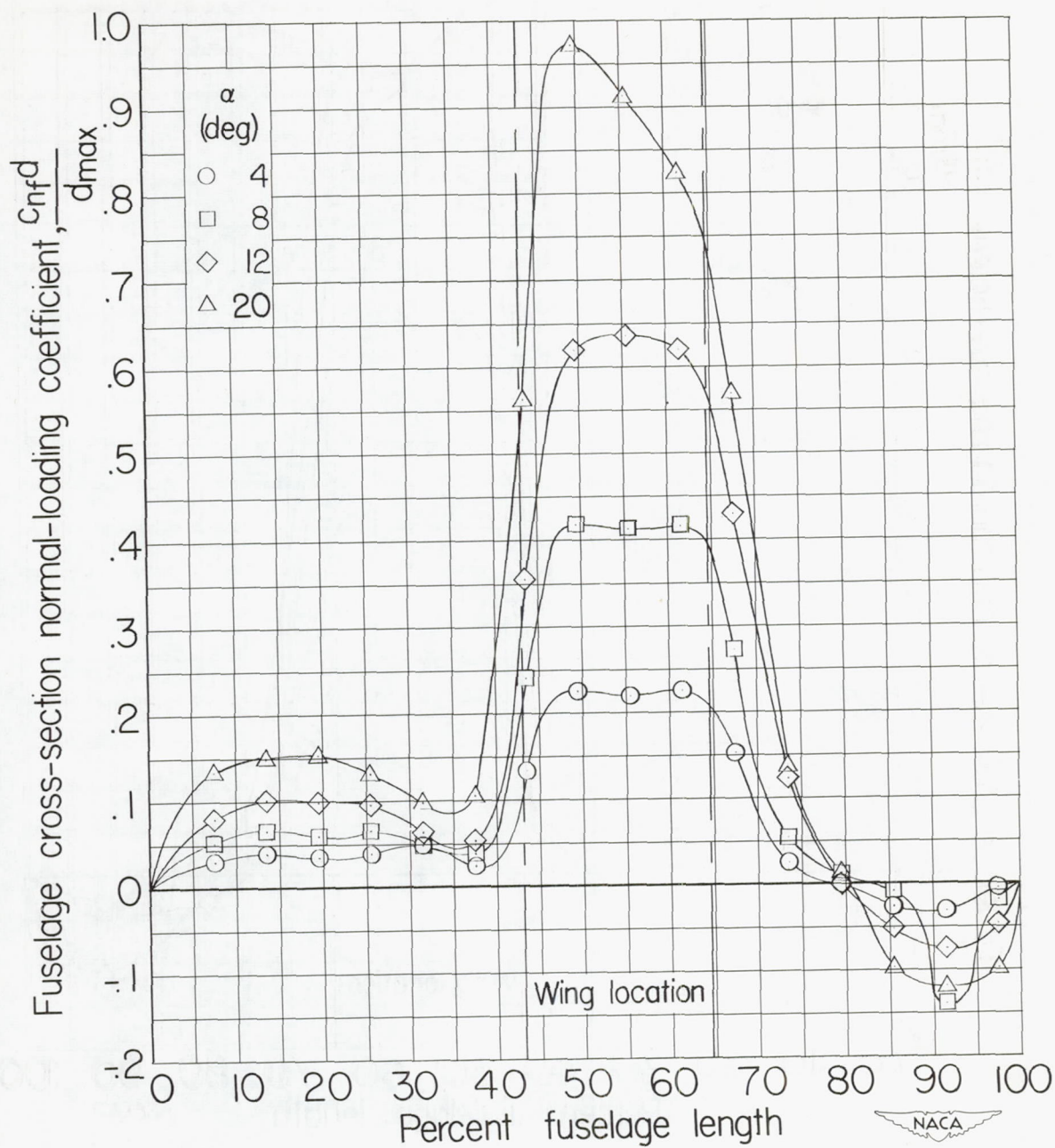
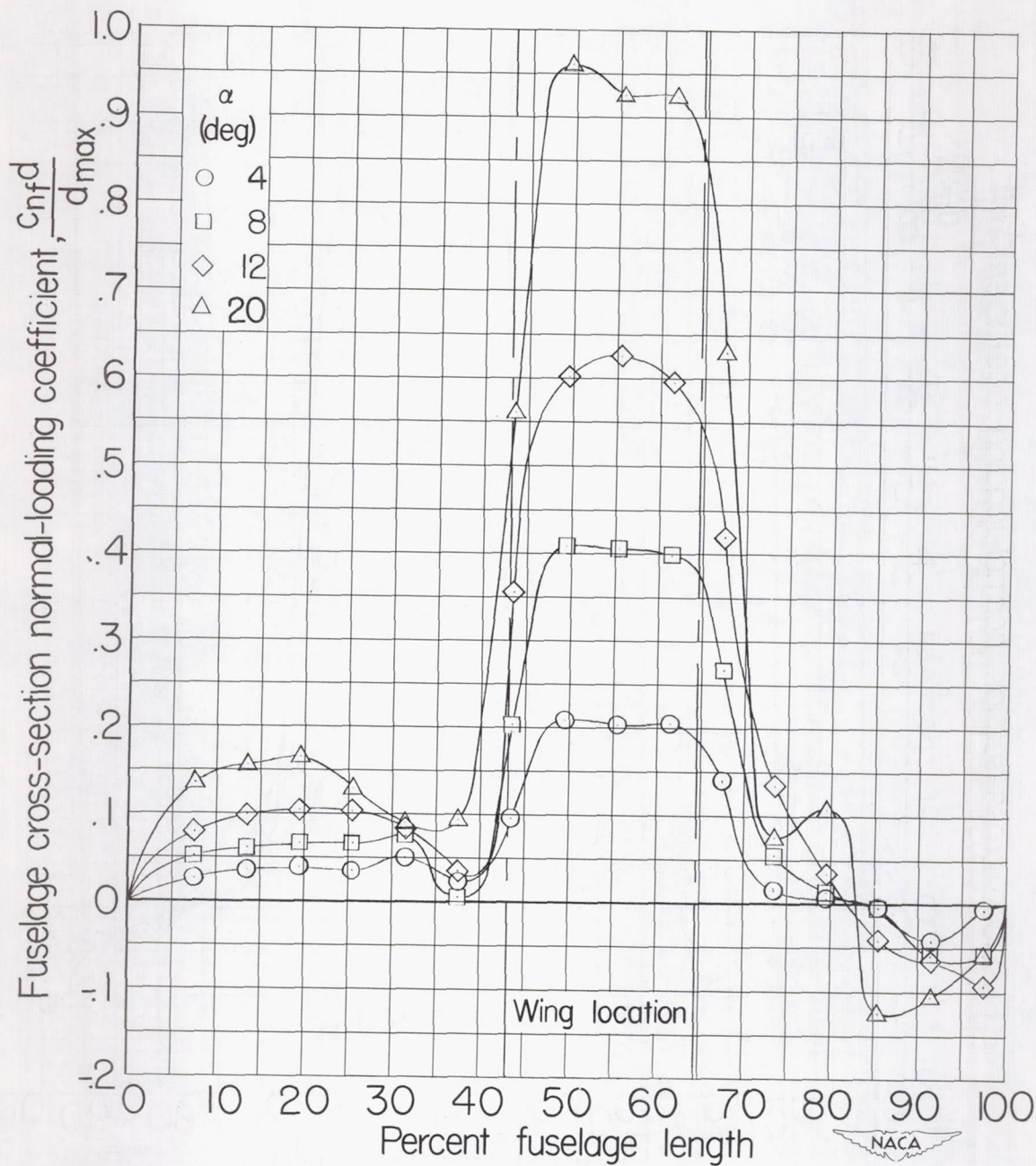
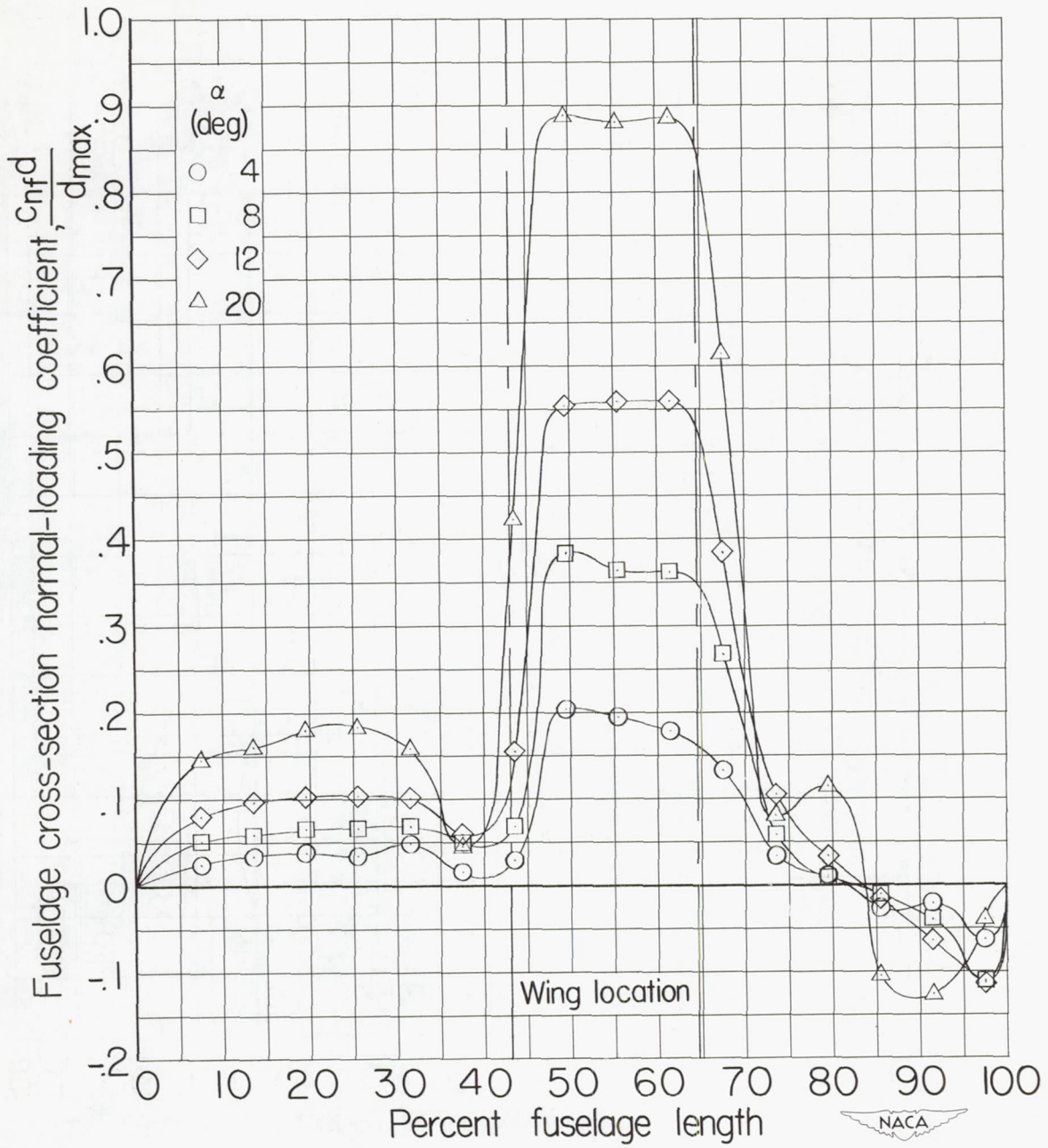
(c)  $M = 0.99$ .

Figure 17.- Continued.



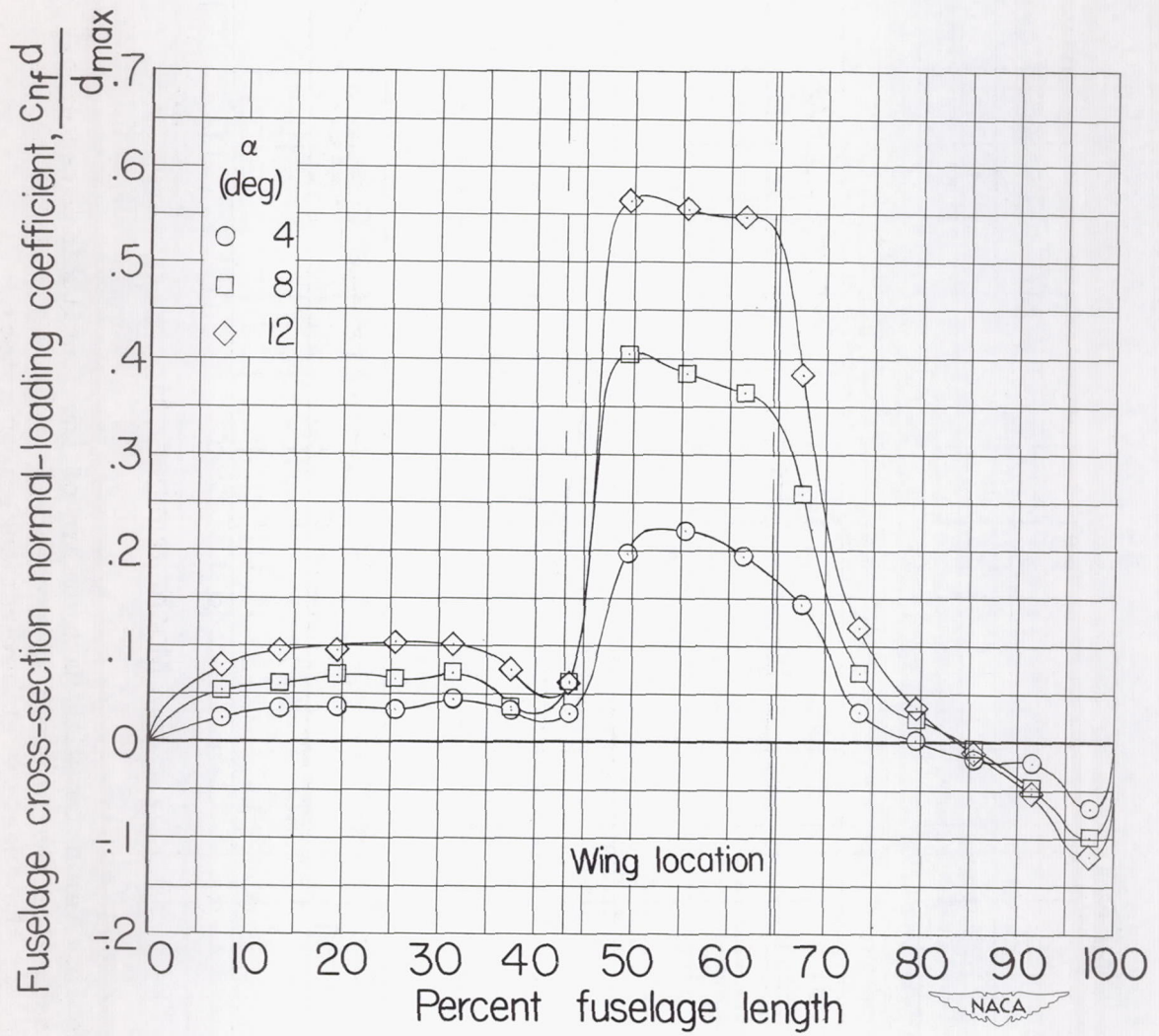
(d)  $M = 1.02$ .

Figure 17.- Continued.



(e)  $M = 1.11$ .

Figure 17.- Continued.



(f)  $M = 1.13$ .

Figure 17.- Concluded.

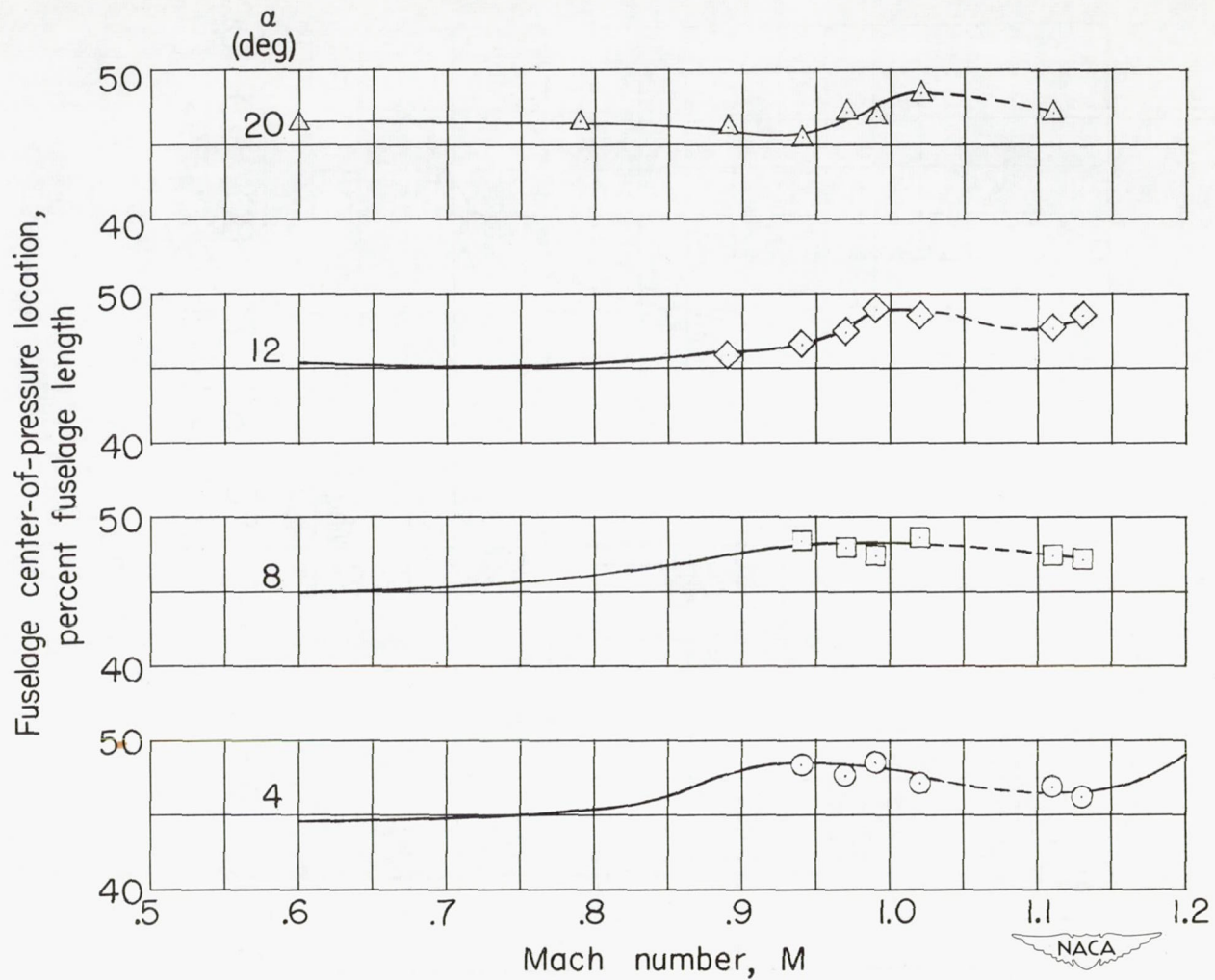


Figure 18.- Variation with Mach number of the longitudinal center of pressure of the fuselage in presence of the wing relative to the nose of the fuselage at several angles of attack.